

# PROJECT REPORT

On

## TRANSFORMING WASTE TO WEALTH: SYNTHESIS, CHARACTERIZATION AND APPLICATIONS OF CELLULOSE NANOCRYSTALS AND CARBON QUANTUM DOTS FROM JACKFRUIT PEELS

Submitted by  
**FEBA GEORGE T.**  
**(AM23CHE006)**

*In partial fulfillment for the award of the  
Post graduate Degree in Chemistry*



DEPARTMENT OF CHEMISTRY  
AND  
CENTRE FOR RESEARCH

ST. TERESA'S COLLEGE (AUTONOMOUS)  
ERNAKULAM

2024-2025

DEPARTMENT OF CHEMISTRY  
AND  
CENTRE FOR RESEARCH

ST. TERESA'S COLLEGE (AUTONOMOUS)  
ERNAKULAM



M.Sc. CHEMISTRY PROJECT REPORT

Name : FEBA GEORGE T.  
Register Number : AM23CHE006  
Year of Work : 2024-2025

This is to certify that the project "TRANSFORMING WASTE TO WEALTH: SYNTHESIS, CHARACTERIZATION AND APPLICATIONS OF CELLULOSE NANOCRYSTALS AND CARBON QUANTUM DOTS FROM JACKFRUIT PEELS" is the work done by FEBA GEORGE T.

Dr. Saritha Chandran A.  
Head of the Department

Dr. Ushamani M.  
Staff-member in charge

Submitted to the Examination of Master's degree in Chemistry

Date: 29/4/2025.....

Examiners: 1. Dr. DEEPA C.S. ....

2. Dr. Roy Keyan Paul. ....

# ISF CHITIN AND MARINE PRODUCTS LLP

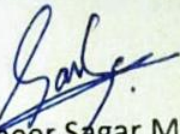
Date: 06-03-2025

## CERTIFICATE

This is to certify that FEBA GEORGE T (Reg.No.-AM23CHE006) a student of Department of Chemistry and Centre for research, St. Teresa's college (Autonomous), Kochi-682011 has successfully completed their project on the topic Transforming waste to wealth: Synthesis,characterization and application of Cellulose nanocrystals and carbon quantum dots from jackfruit peels with support of our company.

We wish all the best in her future academic and professional endeavour's.

For ISF CHITIN AND MARINE PRODUCTS LLP

  
Sameer Sagar M P  
QC Head





ST.TERESA'S COLLEGE (AUTONOMOUS)  
ERNAKULAM



**Certificate of Plagiarism Check for Dissertation**

Author Name

FEBA GEORGE T., NEHA JOSEPH

Course of Study

M.Sc. Chemistry

Name of Guide

Dr. Ushamani M.

Department

Chemistry & Centre For Research

Acceptable Maximum Limit

20

Submitted By

library@teresas.ac.in

TRANSFORMING WASTE TO WEALTH:  
SYNTHESIS, CHARACTERIZATION AND  
APPLICATION OF CELLULOSE NANOCRYSTALS  
AND CARBON QUANTUM DOTS FROM  
JACKFRUIT PEELS

Similarity

3% AI- 7%

Paper ID

3381964

Total Pages

150

Submission Date

2025-03-06 15:04:23

Signature of Student

Signature of Guide

**Dr. Ushamani M**  
Professor

Department of Chemistry & Centre for Research  
St.Teresa's College (Autonomous)  
Ernakulam



Checked By

College Librarian

DEPARTMENT OF CHEMISTRY  
AND  
CENTRE FOR RESEARCH

ST. TERESA'S COLLEGE (AUTONOMOUS)  
ERNAKULAM

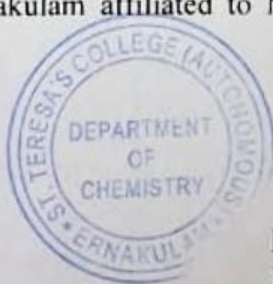


CERTIFICATE

This is to certify that the project work titled "**TRANSFORMING WASTE TO WEALTH: SYNTHESIS OF CELLULOSE NANOCRYSTALS AND CARBON QUANTUM DOTS FROM JACK FRUIT PEELS**" is the work done by **Feba George T.** under the guidance of **Dr. Ushamani M., Professor**, Department of Chemistry and Centre for Research, St. Teresa's College, Ernakulam in partial fulfilment of the award of the Degree of Master of Science in Chemistry at St. Teresa's College, Ernakulam affiliated to Mahatma Gandhi University, Kottayam.

*Ushamani*

Dr. Ushamani M.  
**Dr. Ushamani M**  
Project Guide  
Professor



*Saritha*

Dr. Saritha Chandran A  
Head of the Department

DEPARTMENT OF CHEMISTRY  
AND  
CENTRE FOR RESEARCH

ST. TERESA'S COLLEGE (AUTONOMOUS)  
ERNAKULAM



CERTIFICATE

This is to certify that the project work entitled "**TRANSFORMING WASTE TO WEALTH: SYNTHESIS, CHARACTERIZATION AND APPLICATIONS OF CELLULOSE NANOCRYSTALS AND CARBON QUANTUM DOTS FROM JACK FRUIT PEELS**" is the work done by **FEBA GEORGE T.** under my guidance in the partial fulfilment of the award of the Degree of Master of Science in Chemistry at St. Teresa's College (Autonomous), Ernakulam affiliated to Mahatma Gandhi University, Kottayam.



*Ushamani*

Dr. Ushamani M.

## DECLARATION

I hereby declare that the project work entitled "**TRANSFORMING WASTE TO WEALTH: SYNTHESIS, CHARACTERIZATION AND APPLICATIONS OF CELLULOSE NANOCRYSTALS AND CARBON QUANTUM DOTS FROM JACK FRUIT PEELS**" submitted to Department of Chemistry and Centre for Research, St. Teresa's College (Autonomous) affiliated to Mahatma Gandhi University, Kottayam, Kerala is a record of an original work done by me under the guidance of **Dr. USHAMANI M., PROFESSOR**, Department of Chemistry and Centre for Research, St. Teresa's College (Autonomous), Ernakulam (Internal Guide). This project work is submitted in the partial fulfillment of the requirements for the award of the Degree of Master of Science in Chemistry.



FEBA GEORGE T.

## *Acknowledgements*

---

First of all, I thank **Almighty God** for the successful completion of this project.

I express my heartfelt thanks to my project supervisor **Prof. Dr. Ushamani M.**, our guide, St. Teresa's College (Autonomous), Ernakulam, for her guidance, suggestions and encouragement for the successful completion of this project.

I would also like to express my gratitude to **Mrs. Sicily Rilu Joseph**, Research Scholar, Department of Chemistry, St. Teresa's College, for her continuous guidance and support throughout the project work.

I would like to express my deep sense of gratitude to **Dr. Saritha Chandran A.**, Head of the Department of Chemistry and Centre for Research, St. Teresa's College (Autonomous), Ernakulam, for her constant encouragement and motivations.

I take this opportunity to express my sincere thanks to **Prof. Dr. Alphonsa Vijaya Joseph**, Principal, Manager **Rev. Sr. Nilima** and Directors **Rev. Sr. Francis Ann** and **Rev. Sr. Tessa CSST**, St. Teresa's College (Autonomous), Ernakulam, for being the pillars of support and providing good infrastructure fostering a conductive environment for student's academic growth and development.

I express my heartfelt thanks to **all teachers** of the Chemistry Department, for their wholehearted help and advices during the academic year. I also

---

*Acknowledgements*

remember fondly the valuable support of the **non-teaching staff** of the department during Chemistry Lab and the project hours.

I extend my heartfelt gratitude to **Dr. Vijay John Gerson**, Head of the Department, St. Albert's College (Autonomous), Ernakulam and **Dr. Nisha V.S.**, Assistant Professor, St. Albert's College (Autonomous), Ernakulam for extending academic collaboration and guidance.

I am grateful to **ISF Chitin and Marine Products LLP, Kannamaly** for providing an opportunity for industrial collaboration as part of MSc. Project. The experience and knowledge gained during that time were invaluable and I appreciate the support and guidance provided by the team. The company's willingness to support academic endeavors is truly appreciated.

I heartily thank **TICC** (St. Teresa's College (Autonomous), Ernakulam), **Instrumentation Lab** (Bharata Mata College, Thrikkakara), **SAIF** (Mahatma Gandhi University, Kottayam), **STIC** (CUSAT), **FESEM Laboratory**, Department of Physics, CUSAT, for providing all the spectroscopic assistance needed for the characterization of the samples within the time limit.

Last, but not least, I am grateful to my loving family and friends for the care, support and concern they provide to follow my passion.

*Feba George T.*

## *Contents*

---

<b>Chapter 1 Introduction</b>	<b>1</b>
1.1 Waste to Worth	1
1.2 Cellulose	2
1.2.1 Sources of Cellulose	3
1.3 Composition	5
1.3.1 Cellulose	6
1.3.2 Lignin	7
1.3.3 Hemicellulose	7
1.4 Nanocellulose	8
1.4.1 Characteristics of Nanocellulose	9
1.4.2 Classification of Nanocellulose	10
1.4.2.1 Cellulose Nanocrystals (CNC)	11
1.4.2.2 Cellulose Nanofibers (CNF)	12
1.4.2.3 Bacterial Nanocellulose (BNC)	13
1.4.2.4 Electrospun Cellulose Nanofibers (ECN)	13
1.5 The source – Jackfruit peels	14
1.6 Different methods used for the Extraction of Nanocellulose from Cellulose	16
1.6.1 Acid hydrolysis	16
1.6.2 Enzymatic hydrolysis	18
1.6.3 Mechanical process	19

---

1.7 Pretreatments for the Extraction of Nanocellulose	20
1.7.1 Alkali pulping	21
1.7.2 Bleaching	22
1.8 Acid hydrolysis	22
1.8.1 Mineral acid hydrolysis	22
1.8.2 Organic acid hydrolysis	23
1.9 Applications of Nanocellulose	23
1.9.1 Food packaging industry	24
1.9.2 Biomedical applications	24
1.9.3 Reinforcement in polymer matrix	24
1.9.4 Water purification	25
1.9.5 Papermaking industry	25
1.9.6 Food additives	25
1.9.7 Catalysis	26
1.9.8 Carbon dots	26
1.10 Chitin and Chitosan	27
1.10.1 Properties of Chitosan	28
1.10.2 Application of Chitosan	29
1.11 Quantum Dots	30
1.11.1 Types of Quantum Dots	30
1.11.2 Carbon Quantum Dots	31
1.12 Fluorescent Ink	32
1.13 Antioxidant Analysis	32
1.14 Objectives	33
<b>Chapter 2 Review of Literature</b>	<b>35</b>

---

<b>Chapter 3 Materials and Methods</b>	<b>47</b>
3.1 Introduction	47
3.2 Synthesis of Cellulose Nanocrystals (CNC) from Jackfruit peels	47
3.2.1 Chemicals required	47
3.2.2 Materials required	47
3.2.3 Apparatus required	48
3.2.4 Synthesis of Cellulose Nanocrystals (CNC)	48
3.2.4.1 Alkali pulping	49
3.2.4.2 Bleaching	49
3.2.4.3 Acid hydrolysis	50
3.3 Extraction of Chitosan from Shrimp shells	51
3.3.1 Materials required	51
3.3.2 Extraction of Chitin	52
3.3.3 Extraction of Chitosan from Chitin	52
3.4 Determination of Ash and Moisture content of Chitin and Chitosan	52
3.4.1 Materials Required	52
3.5 Determination of Viscosity and Degree of Deacetylation (DDA) of Chitosan	53
3.5.1 Materials required	53
3.6 PVA /Chitosan/ CNC film	54
3.6.1 Chemicals required	54
3.6.2 Materials required	55
3.6.3 Apparatus required	55
3.6.4 Preparation of PVA/Chitosan/CNC Nanocomposite Film	55

---

3.7 Synthesis of Carbon Quantum Dots	56
3.7.1 Hydrothermal method	56
3.8 Antioxidant Analysis	57
3.9 Carbon Quantum Dot-based Fluorescent Ink Formulation	57
3.10 Cellulose Paper	57
3.10.1 Materials required	58
3.10.2 Apparatus required	58
3.10.3 Preparation of Cellulose Paper	58
3.11 Characterization techniques	58
3.11.1 X- Ray Diffraction (XRD)	58
3.11.2 Fourier Transform Infrared Spectroscopy (FTIR)	59
3.11.3 Scanning Electron Microscopy (SEM)	60
3.11.4 Transmission Electron Microscopy (TEM)	61
3.11.5 Thermogravimetric (TGA) Analysis	62
3.11.6 Mechanical Properties (Tensile Strength)	63
3.11.7 UV- Visible Spectroscopy	64
3.11.8 Photoluminescence Spectroscopy	65
<b>Chapter 4 Results and Discussion</b>	<b>66</b>
4.1 Characterization of Cellulose Nanocrystals (CNC)	66
4.1.1 Physical Appearance	66
4.1.2 X-Ray Diffraction (XRD)	67
4.1.3 Fourier Transform Infrared Spectroscopy (FTIR)	68
4.1.4 Field Emission Scanning Electron Microscopy (FESEM)	69
4.1.5 Transmission Electron Microscopy (TEM)	70

---

4.1.6 Thermogravimetric and Derivative Thermogravimetric Analysis (TGA)	71
4.2 Determination of Ash and Moisture content of Chitin and Chitosan	73
4.3 Determination of Viscosity and Degree of Deacetylation (DDA)	74
4.4 Characterization of PVA/Chitosan/CNC Nanocomposite Film	75
4.4.1 Fourier Transform Infrared Spectroscopy (FTIR)	75
4.4.2 Field Emission Scanning Electron Microscopy (FESEM)	76
4.2.3 Mechanical Properties (Tensile Strength)	77
4.5 Applications of PVA/Chitosan/CNC Nanocomposite films	78
4.5.1 Impact of PVA/Chitosan/CNC film on Curry Leaf Freshness and Shelf Life	78
4.5.2 Application of PVA/Chitosan/CNC Nanocomposite Film in Hydrocarbon removal and Oil spill remediation	81
4.6 Cellulose Paper	84
4.7 Characterization techniques of Carbon Quantum Dots	84
4.7.1 UV-Vis Spectroscopy	84
4.7.2 Photoluminescence Spectroscopic Technique	85
4.8 Applications of Carbon Quantum Dots	86
4.8.1 Antioxidant Analysis	86
4.8.2 Fluorescent Ink	87
<b>Chapter 5 Conclusion</b>	<b>88</b>
<b>References</b>	<b>94</b>
<b>Papers published/ Presented</b>	<b>110</b>

## **List of Tables**

Table 4.1	Moisture and Ash content of Chitin & Chitosan
Table 4.2	DO value of water from the three sampling stations
Table 4.3	Hydrocarbon concentration of the collected water samples

## **List of Diagrams**

Figure 1.1	The 3R hierarchy – ‘Reduce, Reuse, Recycle’
Figure 1.2	Structure of Cellulose
Figure 1.3	Plant cell wall
Figure 1.4	Sources of Cellulose (a)
Figure 1.5	Sources of Cellulose (b)
Figure 1.6	Components of Lignocellulosic biomass (LB)
Figure 1.7	Schematic representation of Nanocellulose present in plant cell wall
Figure 1.8	Characteristics of Nanocellulose
Figure 1.9	Classification of Nanocellulose
Figure 1.10	Synthesis of Cellulose Nanocrystals (CNC) through Acid hydrolysis
Figure 1.11	Synthesis of Cellulose Nanofibre (CNF)
Figure 1.12	Synthesis of Bacterial Nanocellulose (BNC)
Figure 1.13	Synthesis of Electrospun Cellulose Nanofibres (ECN)
Figure 1.14	(a) Jackfruit (b) Jackfruit peels
Figure 1.15	Acid hydrolysis of Cellulose yielding Cellulose nanocrystals (CNC)
Figure 1.16	Enzymatic hydrolysis
Figure 1.17	Mechanical treatment of Cellulose
Figure 1.18	Effect of Pre-treatments

Figure 1.19	Isolation of Cellulose Nanocrystals (CNC) from waste biomass
Figure 1.20	Applications of Nanocellulose
Figure 1.21	Structures of (a) Chitin (b) Chitosan
Figure 3.1	a) Dried Jackfruit peels (b) Jackfruit peel powder.
Figure 3.2	Alkali pulping
Figure 3.3	Bleaching
Figure 3.4	Acid hydrolysis
Figure 3.5	Flow chart showing the synthesis of Cellulose Nanocrystals
Figure 3.6	Preparation of PVA/Chitosan/CNC Nanocomposite Film
Figure 4.1	a) Raw Material , (b) Cellulose , (c) Cellulose Nanocrystals (CNC)
Figure 4.2	XRD spectra of Raw material, extracted Cellulose and Cellulose Nanocrystals (CNC)
Figure 4.3	FTIR spectra of Raw material, extracted Cellulose and Cellulose Nanocrystals (CNC)
Figure 4.4	FESEM Images of (a) Raw material, (b) Cellulose, (c) Cellulose Nanocrystals (CNC)
Figure 4.5	TEM image of Cellulose Nanocrystals (CNC)
Figure 4.6	TGA-DTA of (a) Raw material (b) Cellulose Nanocrystals (CNC)
Figure 4.7	FTIR spectra of PVA/Chitosan and PVA/Chitosan/CNC Nanocomposite Films
Figure 4.8	FESEM Images of (a) PVA/CS and (b) PVA/CS/1% CNC Nanocomposite Films
Figure 4.9	Visual comparison of Curry leaves over 57 hours Unwrapped leaves and leaves wrapped in PVA/Chitosan/1% CNC Nanocomposite Film
Figure 4.10	Visual comparison of Curry leaves over 57 hours wrapped in Nanocurcumin Nanocomposite Film and leaves wrapped in Lemon Grass oil Nanocomposite Film

*Contents*

---

Figure 4.11	Printable Cellulose Paper
Figure 4.12	UV-Vis Spectra of Carbon Quantum Dot
Figure 4.13	Photoluminescence Spectra of Carbon Quantum Dot

## **Abbreviations**

CNC	Cellulose Nanocrystals
CNF	Cellulose Nanofibres
BNC	Bacterial Nanocellulose
ECN	Electrospun Cellulose Nanofibre
CS	Chitosan
DDA	Degree of Deacetylation
QD	Quantum Dots
CQD	Carbon Quantum Dot
PVA	Polyvinyl alcohol
FTIR	Fourier Transform Infrared Spectroscopy
XRD	X-ray Diffraction
FESEM	Field Emission Scanning Electron Microscopy
TEM	Transmission Electron Microscopy
TGA	Thermogravimetric Analysis

# Chapter 1

## INTRODUCTION

### 1.1 WASTE TO WORTH

One of the major issues that our world face today is waste management which is essential for a sustainable living. In such a scenario, the ‘Reduce, Reuse, Recycle (R-R-R)’ principle as in Fig.1.1 becomes relevant. ‘Reduce’ aims to mitigate the amount of waste generated every year by choosing renewable and sustainable products. The environmental impact of wastes can be lessened by making public aware of the subsequent consequences and thereby making them to rethink their excessive purchasing habits and adopt a sustainable living. ‘Reuse’ emphasizes the utilization of waste and unwanted substances in day-to-day life and use it as an alternative to the existing materials instead of discarding it as a waste. ‘Recycle’ is a means of converting already used materials to valuable products, so that they can be used for future needs [1]. Jackfruit (*Artocarpus heterophyllus*) is a species of tree that is widely found in Southeast Asia and Pacific region [2]. It belongs to the Moraceae family. Usually we consume jackfruit and discard its peels as a waste because it is inconsumable. Even though the peels are biodegradable, it piles up as agro-waste. It can lead to the production of greenhouse gases, suffocation due to pungent odors because of its decay, as well as water pollution [3]. So keeping these two in mind we came across an idea of transforming this waste into worth by the synthesis of nanocellulose and carbon quantum dots from jackfruit peels. The key concept of our work is ‘Waste to

Wealth'. It refers to the process of transformation of waste materials into valuable products or resources. This initiative plays a crucial role in promoting sustainable waste management, minimizing environmental pollution and driving economic growth.



**Fig.1.1: The 3R hierarchy – ‘Reduce, Reuse, Recycle’ [4]**

## **1.2 CELLULOSE**

Cellulose stands out as an ideal choice for sustainable material development. It is a complex carbohydrate with molecular formula  $(C_6H_{10}O_5)_n$  as in Fig 1.2. It is the most abundant organic compound on Earth. It is present in the cell walls of plants and algae. They are joined by D- glucopyranosyl units via by  $\beta$ -1, 4 -glycosidic bonds [5]. They are highly crystalline, insoluble in water, renewable and biodegradable. Through photosynthesis, plants synthesize cellulose [6]. It is comprised of plasma membrane, hemicellulose, pectin etc as shown in Fig. 1.3.

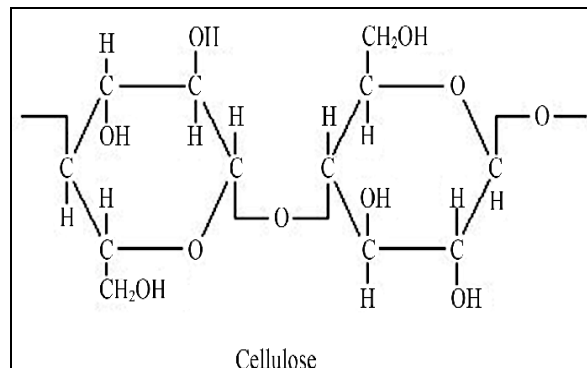


**Fig.1.2: Structure of Cellulose [7]**

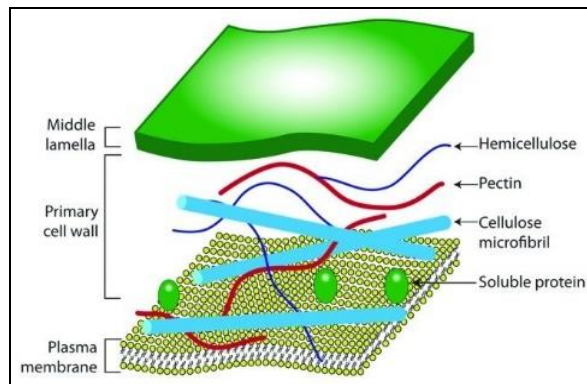


**Fig.1.3: Plant cell wall [8]**

### 1.2.1 Sources of Cellulose

There are natural as well as synthetic sources of cellulose. The primary source of cellulose is the plant cell wall. Natural fibres are extracted from cotton, jute, flax, ramie, sisal, hemp etc. Synthetic fibres are derived from fabrics like Lyocell, modal, rayon etc. [9]. Fig.1.4 (a) shows the different sources of cellulose.

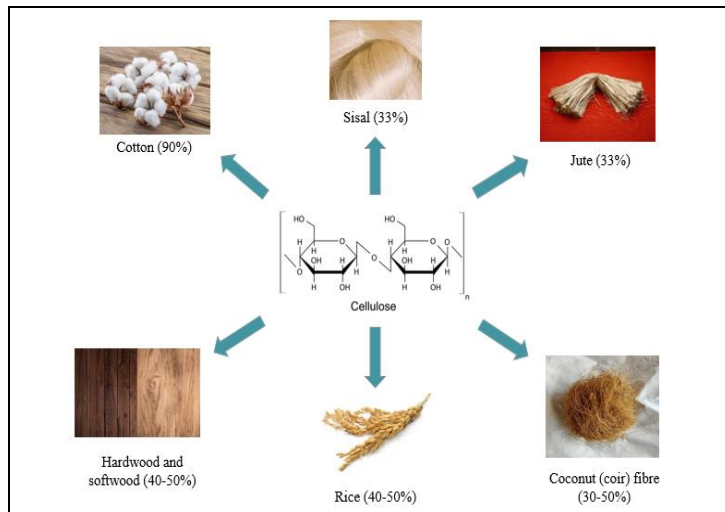


**Fig1.4: Sources of Cellulose (a)**

There are lignocellulosic sources, animal, algae and bacterial sources as shown in Fig.1.5 (b).

- i. The lignocellulosic sources can be divided into two [10]:
  - a. Woody residues : Hardwood, softwood [11] and sawdust wastes [12]
  - b. Non-woody plants and agricultural residues: Kenaf [13], corn husk [14], bamboo [15], watermelon rind and water hyacinth [16], sugarcane bagasse [17], [18], [19] etc.
- ii. Animal sources: Tunicates like *Halocynthia papillosa* [20], *Halocynthia roretzi* [21], *Styela plicata* [22] etc.
- iii. Algae (red, green, grey, yellow-green etc.): *Cladophorales* and *Siphonocladales* are the orders of algae that produce cellulose. *Cladophorales* include *Cladophora* [23], *Chaetomorpha* [24], *Rhizoclonium* [25] etc. and *Siphonocladales* include *Valonia* [26], *Dictyosphaeria* [27] etc. *Gelidium* red algae is another example [10].
- iv. Bacteria: *Acetobacter xylinus*, *Agrobacterium*, *Seudomonas*, *Rhizobium* and *Sarcina* are examples of cellulose producing bacteria's. *Acetobacter*

*xylinum* which is a Gram negative acetic acid bacteria is the most dominant among these to produce cellulose. [10]

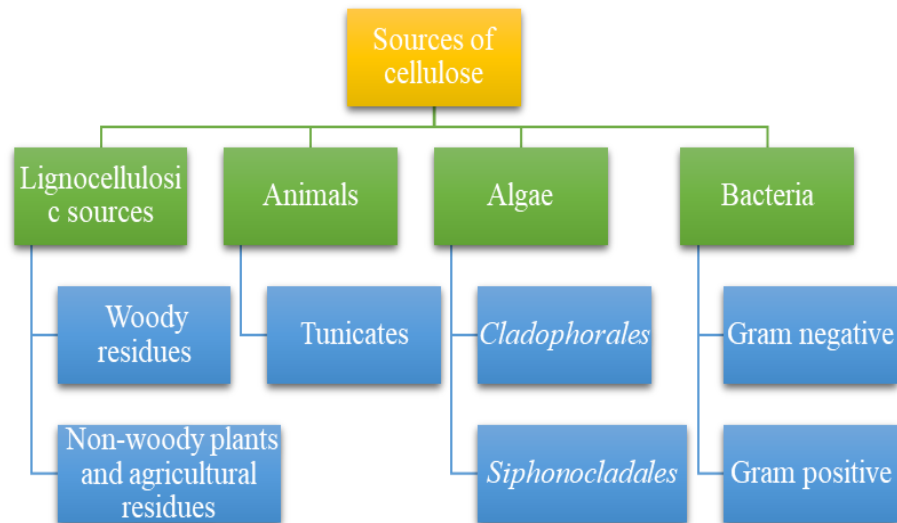


**Fig.1.5: Sources of Cellulose (b)**

### 1.3 COMPOSITION

Cellulosic Nanocrystals (CNCs) can be effectively segregated and purified from the complex matrix of Lignocellulosic Biomass (LB) using specialized techniques. Lignocellulosic Biomass (LB) is a plant-derived material characterized by its heterogeneous composition, comprising of the polysaccharides like hemicelluloses and cellulose as well as lignin, a complex aromatic biopolymer as in Fig.1.6 [28].

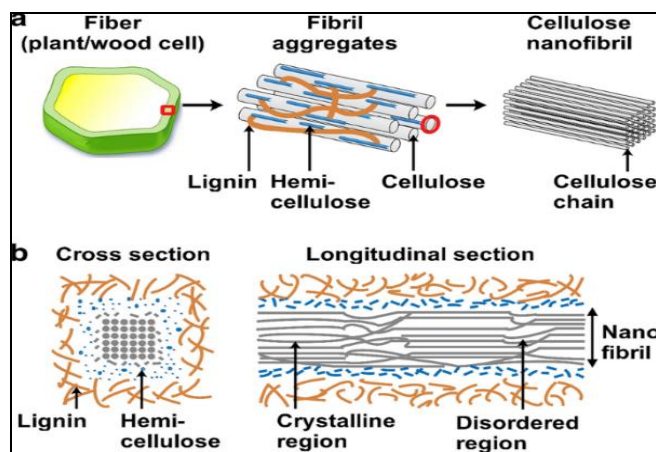


**Fig.1.6: Components of Lignocellulosic**

**biomass (LB) [29]**

### 1.3.1 Cellulose

Although the Earth generates more than thousand tons of cellulose each year, a mere 5% is currently extracted and utilized in diverse products. In 1838, Anselme Payen successfully extracted cellulose from LB via nitric acid treatment and determined its molecular composition as  $C_6H_{10}O_5$ . Notably, the term "cellulose" was first formally articulated within the scientific community in 1839 [28].

Cellulose is a homopolymer. It is entirely made up of glucose and no other sugar unit is present. It is the main structural element of plant cell wall. Depending on its source and type of processing, cellulose shows variability in its degree of polymerization. But in general it exhibits higher degree of polymerization [30].

Native cellulose, produced by plants, exists in two main crystalline forms: cellulose I and cellulose II, with cellulose II commonly found in marine algae and formed by treating cellulose I with sodium hydroxide. Among

cellulose's four crystalline polymorphs - I, II, III, and IV - cellulose II exhibits the highest thermodynamic stability, whereas cellulose I is relatively less stable. Notably, liquid ammonia treatment of cellulose I and II results in the formation of crystalline cellulose III, which subsequently transforms into cellulose IV upon heating [9].

### **1.3.2 Lignin**

Native lignin, also referred to as protolignin, is a complex, three-dimensional, crosslinked macromolecule biosynthesized from the polymerization of three primary phenylpropanoid precursors: Coniferyl alcohol, paracoumaryl alcohol and sinapyl alcohol. The specific proportions of these precursors vary significantly depending on the species, source, and type of lignocellulosic biomass (LB). This variability influences the structural and functional properties of lignin. Lignin acts as a binding agent in cell tissues, holding cellulose and hemicellulose fibers together. As plant cell walls mature, lignin provides stiffness and rigidity. Lignin contributes to the water resistance and impermeability of plant cell structures, protects plants against pathogens and environmental stresses. Lignin's complex structure and functionality make it an essential component of plant cell walls, providing strength, stability, and resistance to degradation [28].

### **1.3.3 Hemicellulose**

The term "hemicellulose" was first coined by Schulze to describe polysaccharides extractable from lignocellulosic biomass (LB) using dilute alkali and readily hydrolyzable by dilute acids. Hemicelluloses comprise 15-35% of LB and are the second most abundant constituent

after cellulose. These non-crystalline polysaccharides exhibit complex structures comprising various derivatives of pentoses (arabinose and xylose), hexoses (galactose, fucose, glucose, mannose, and rhamnose), and glycolytic acid (glucose fermentation acid, methyl-glucose and galacturonic acid). The primary sugar units in hemicelluloses are xylans and glucomannans. Hemicelluloses adhere to cellulose through van der Waals and hydrogen bonding and form strong cross-links with lignin. By integrating between cellulose and lignin, hemicelluloses play a vital role in maintaining cell wall structure. Hemicelluloses can be removed from lignocellulosic biomass (LB) through pretreatment methods such as alkali, dilute acid, or steam explosion [28].

#### **1.4 NANOCELLULOSE**

Nanocellulose refers to the cellulose material possessing at least one dimension within the nanoscale range of 1-100 nanometers [31]. Properties like low density, flexibility, high strength, chemical inertness etc. contribute towards its outstanding applications [28].

Low density of nanocellulose makes it lightweight. High aspect ratio, strength etc contributes to its potential as a reinforcing agent. The surface of nanocellulose is ample with hydroxyl bonds which in turn promote hydrogen bonding. CNC has the ability to self-assemble into chiral nematic liquid crystalline phase. Their potential in packaging applications is liable to their low-porosity [32]. Fig.1.7. represents the schematic representation of Nanocellulose present in plant cell wall.



**Fig.1.7: Schematic representation of Nanocellulose present in plant cell wall [33]**

#### **1.4.1 Characteristics of Nanocellulose**

Cellulose researchers have noted that plant and crop cellulose is made of millimeter-sized fibers, which in turn are made of increasingly denser microfibers. These microfibers further consist of nanometer-sized microfibrils that form the basic building blocks of cellulose from different sources. Scientists realized the potential of these nanosized microfibrils, which have vast surface areas and strong bonding capacities, to create innovative products with significantly enhanced strength and functionality [34]. Nanocellulose holds a remarkable number of properties and, thus, is quite versatile in diverse applications. Its mechanical strength, large specific surface area, and stiff structure provide great potential in reinforcing composite applications and making it chemically modifiable. In addition to these beneficial properties, nanocellulose's biocompatibility and biodegradability coupled with its very good barrier properties as well

as its ability to form stable gels and emulsions open wide windows for even more extensive uses in the biomedical, environmental, packaging, and drug delivery sectors [6]. Fig.1.8 shows the different characteristics of nanocellulose.

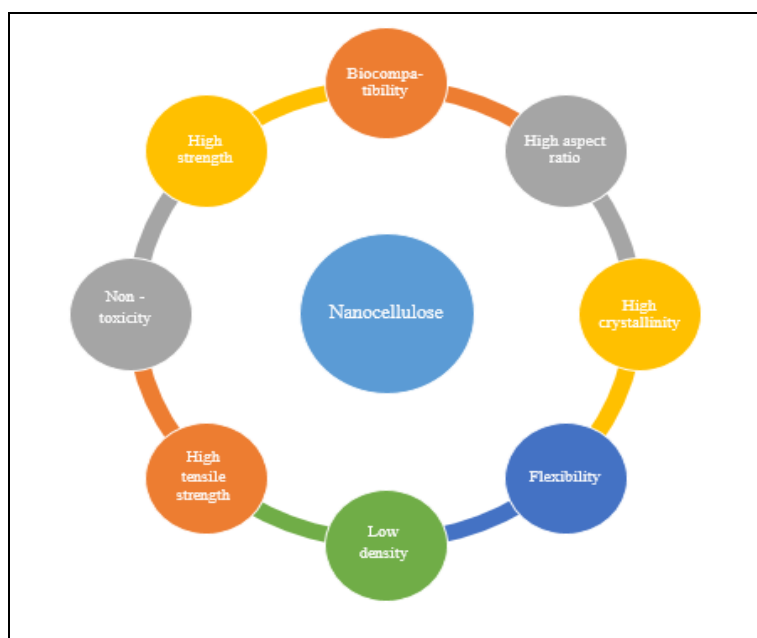


**Fig.1.8: Characteristics of Nanocellulose**

#### 1.4.2 Classification of Nanocellulose

Nanocellulose is divided into four: cellulose nanocrystals (CNC)/ cellulose whiskers, cellulose nanofibres (CNF), bacterial nanocellulose (BNC) and Electrospun Cellulose Nanofiber (ECN). Cellulose nanocrystals (CNC) can be prepared using acid hydrolysis whereas Cellulose nanofibrils (CNF) production usually involves chemical pretreatment and subsequent mechanical disintegration through homogenization, microfluidization, or super-grinding. The dimensions of

cellulose nanocrystals (CNC) typically ranges a few nanometers in diameter and 10-500 nanometers in length, whereas cellulose nanofibrils (CNFs) have diameters ranging from 3-50 nanometers and lengths up to several micrometers [28]. Rice husk, wheat straw, sugarcane bagasse pulp, wood pulp, cotton linters, bacterial cellulose, algal cellulose etc are the various sources of nanocellulose [35].

Cellulose nanostructured materials is comprised of four main classes: Cellulose nanofibrils (CNF), cellulose nanocrystals (CNC)/ cellulose whiskers, bacterial nanocellulose (BNC) and Electrospun cellulose Nanofiber (ECN) [31] as shown in Fig.1.9.

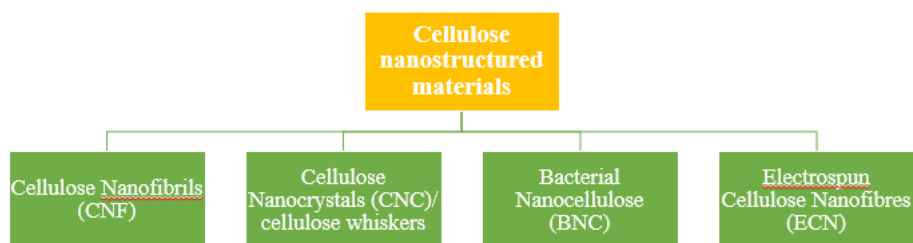


**Fig.1.9: Classification of Nanocellulose**

#### **1.4.2.1 Cellulose Nanocrystals (CNC)**

Cellulose Nanocrystals (CNCs) have a distinctive rod shape or needle-like structure, exhibiting a high crystallinity along with retaining some disordered amorphous regions. Through acid hydrolysis as shown in Fig.1.10, amorphous regions are selectively dissolved, thereby resulting in the extraction of cellulose nanocrystals. The synthesized CNCs exhibit a diameter of 5 nm and their length ranges from 20 to 100 nm [31].

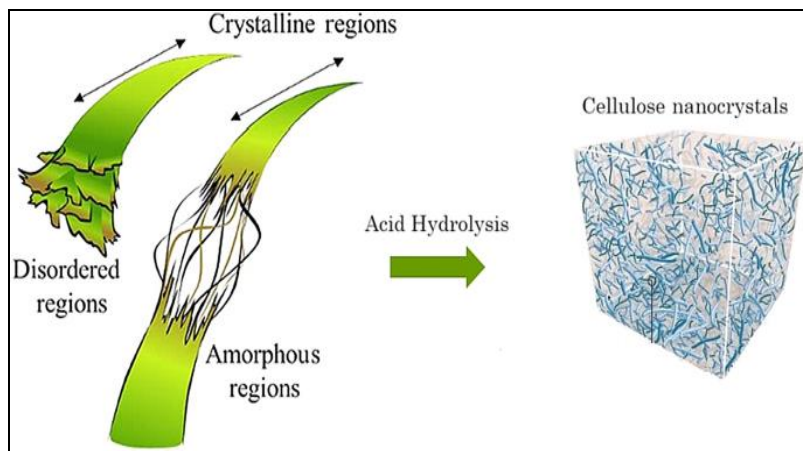


**Fig.1.10: Synthesis of Cellulose nanocrystals (CNC) through acid hydrolysis [36]**

#### 1.4.2.2 Cellulose Nanofibres (CNF)

Cellulose nanofibrils are nanoscale cellulose fibers. They exhibit diameters between 5-60 nm and lengths upto several microns. These fibrils comprised of both crystalline and amorphous regions. They are typically extracted from wood pulp using the TEMPO-mediated oxidation method [31]. Fig.1.11. shows the synthesis of cellulose nanofibres (CNF) from wood pulp.

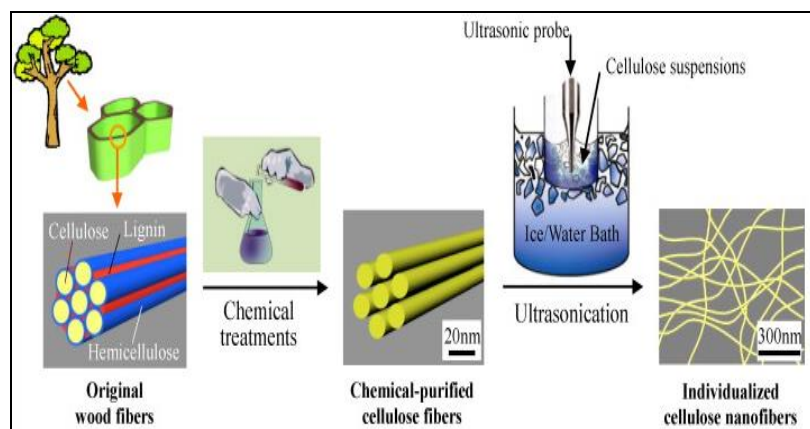


**Fig.1.11: Synthesis of Cellulose nanofibre (CNF) [37]**

#### 1.4.2.3 Bacterial Nanocellulose (BNC)

Bacterial Nanocellulose (BNC) exhibits a ribbon-shaped morphology with dimensions ranging from 20-100 nm and many micrometers in length. Fermentation by specific bacterial genera like *Rhizobium*, *Agrobacterium*, *Gluconacetobacter*, and *Sarcina* generates Bacterial nanocellulose (BNC) as an extracellular product. The purity of BNC makes it stand apart, lacking unwanted plant-derived polymers that are commonly present in traditional plant based cellulose sources [31]. Fig.1.12 shows the synthesis of bacterial nanocellulose (BNC).

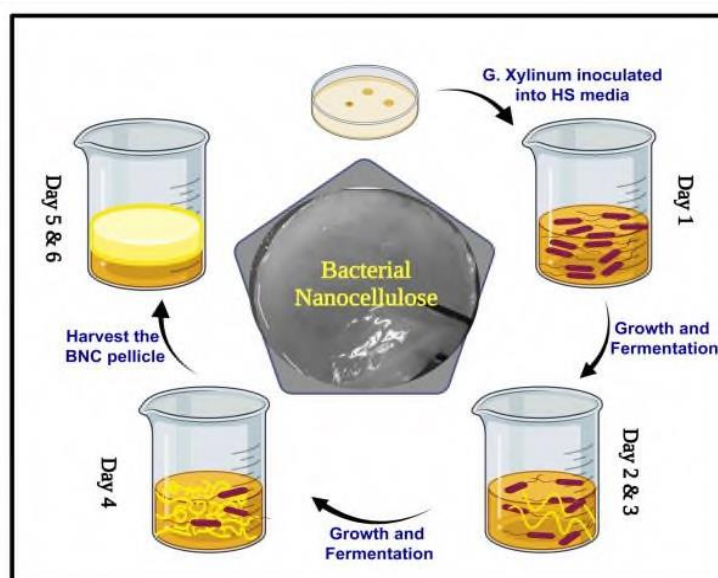


**Fig.1.12: Synthesis of Bacterial nanocellulose (BNC) [38]**

#### 1.4.2.4 Electrospun Cellulose Nanofiber (ECN)

Ultrathin fibres having diameters in the nanometer ranges can be produced using electrospinning. Electrospun fibres can be engineered according to

our interest so that it can be used in many applications. Electrospinning is a method of electrohydrodynamics whereby an electrified liquid droplet experiences elongation into a filament via jet formation, followed by later stretching and elongation. This technique utilizes high voltage on a solution or a melt of polymer; the resultant charged jet elongates and solidifies during the travel toward a collector. The fiber has large surface area-to-volume ratios with directional porosity and better mechanical properties [39]. Fig.1.13. shows the synthesis of electrospun cellulose nanofibres (ECN).

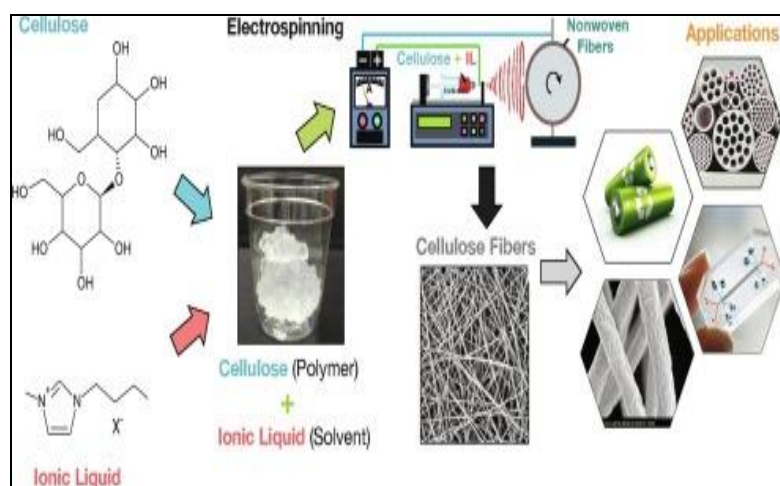


**Fig.1.13: Synthesis of Electrospun Cellulose nanofibres (ECN) [40]**

#### 1.4 THE SOURCE – JACKFRUIT PEELS

The Jackfruit (*Artocarpus heterophyllus*) tree as shown in Fig.1.14 (a) belongs to the mulberry family (Moraceae). It is known as Palaa (Tamil), Chakka (Malayalam), Kanthal (Bengali) etc., in regional languages. It is also known by the names *Artocarpus brasiliensis* Gomez, *Artocarpus*

*heterophylla* Lam., *Artocarpus maxima* Blanco etc. Even though it is native to Western Ghats in India, it is also found in Florida, Brazil, Puerto Rico etc. It produces the biggest known consumable fruit Jackfruit (upto 35 Kg). It has applications in pharmacology, it shows anti-inflammatory effect, antioxidant effect, antifungal effect etc., making it an excellent choice as source material [41]. Each year, a single tree bears 200-500 fruits such as each fruit weighs around 23-40 Kg. A single jackfruit tree yields jackfruit peels around 2714–11800 kg annually, thereby acting as a waste. Jackfruit peels consists of non-cellulosic components like lignin, hemicellulose etc., along with cellulose. Researches have been done considerable work in utilizing fruit, leaves, seeds etc., but much research haven't been done to utilize these jackfruit peels which are considered inedible and as an agro-waste [42]. Raj et.al have reported  $21.29 \pm 1.90$  % yield for cellulose from jackfruit peels which highlights its ability to be used as a source of cellulose [43].

Jackfruit peels as in Fig.1.14 (b) are considered as an agro waste. But they can be recycled in various methods to contribute to sustainability. They can be repurposed as organic fertilizers. They can be processed into nutrient enriched cattle feed. Jackfruit peels are rich in bioactive compounds such as polyphenols and pectin, which can find its application in pharmaceutical industry. The cellulose and hemicellulose in jackfruit peels can be used to produce biofuels such as ethanol and butanol. They can be used in wastewater treatment applications by serving as a bio-based coagulating agents [44].

In the context of global environmental concerns and the urgent need for sustainable materials, researchers are increasingly looking toward natural, renewable resources to replace conventional, non-biodegradable options.

Hence our work focusses on the extraction of cellulose from jackfruit peels and the synthesis of Cellulose Nanocrystals (CNC) from cellulose [34].



**Fig.1.14: (a) Jackfruit (b) Jackfruit peels**

## **1.6 DIFFERENT METHODS USED FOR THE EXTRACTION OF NANOCELLULOSE FROM CELLULOSE**

### **1.6.1 Acid Hydrolysis**

The acid-hydrolysis process of cellulose transforms it into smaller sugars, mainly glucose. It involves the cleavage of  $\beta$ -1, 4-glucosidic bonds of cellulose chains so that shorter chain fragments are created. Hydrolysis is generally influenced by the presence of other factors such as acid concentration, temperature, and the kinds of structural forms of cellulose. Acid concentration is the most influential because it constitutes a very crucial factor for the kinetics and mode of hydrolysis. For example, the sulfuric acid amounts are varied considerably, depending on the procedure for hydrolysis.

There is another factor, namely temperature, which brings about different rates of occurrences and yields in hydrolysis according to the temperature. Cellulose at this temperature degrades into oligosaccharides and further

hydrolysis to glucose at the indicated higher temperatures at about 30°C in 40% hydrochloric acid.

An important aspect is the cellulose acid complex formation during acid hydrolysis, caused by the partial destruction of the crystalline structure of cellulose when concentrated acid reaches the level of effective hydrolysis. Kinetics of acid hydrolysis are complex and have been widely studied. Many kinetic equations have been proposed to describe hydrolysis of cellulose and oligosaccharides in different conditions. Chemical modifications include acid hydrolysis decreasing the average degree of polymerization of cellulose and introducing reactive groups in the polymer to improve the reducing power of cellulose. Acid hydrolysis of cellulose is a complex process. It will help in several applications, such as biofuel [45]. Fig 1.15 represents the acid hydrolysis of cellulose.

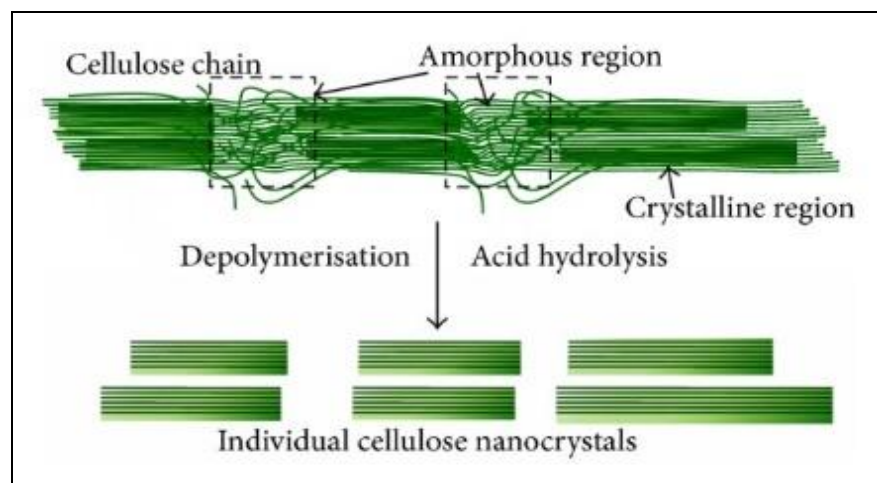


**Fig.1.15: Acid hydrolysis of Cellulose yielding Cellulose nanocrystals (CNC) [46]**

### 1.6.2 Enzymatic Hydrolysis

Enzymatic hydrolysis breaks down cellulose at the solid-liquid interface through a series of steps. The process is largely carried out by enzymes known as glycosyl hydrolases, of which endoglucanases and exoglucanases/cellobiohydrolases are primarily included. These enzymes, collectively, degrade cellulose to smaller soluble products such as cellobiose and celluloooligosaccharides, which are further hydrolyzed by  $\beta$ -glucosidase to glucose. The physical properties of cellulose and the unique modes of action of enzymes influence enzymatic hydrolysis efficiency. Increasing enzyme access and activity involve factors such as biomass pretreatment, which alters the physical and chemical properties of cellulose. The physical properties of cellulose and the unique manner in which enzymes act influence the efficiency of enzymatic hydrolysis. Increasing enzyme accessibility and activity necessitates conditions such as biomass pretreatment, which alters the physical and chemical properties of cellulose [47]. Schematic representation of enzymatic hydrolysis is as shown in Fig. 1.16.

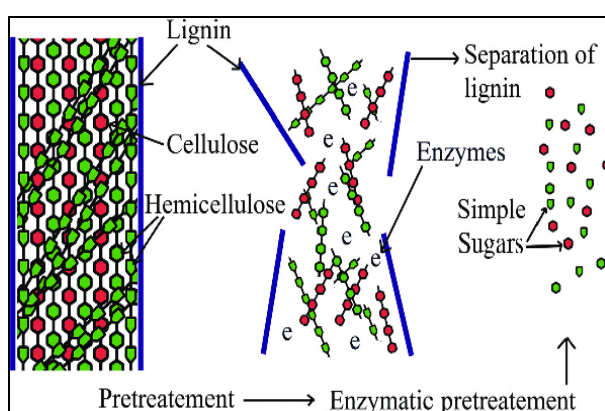


**Fig.1.16: Enzymatic hydrolysis [48]**

### **1.6.3 Mechanical Process**

Mechanical pretreatments, as shown in Fig.1.17, as a step in cellulose modification before acid hydrolysis in the synthesis route, are therefore of great significance as this leads to effective and efficient strategies for CNCs production. Researchers have evaluated various mechanical pretreatment techniques (magnetic agitation, milling, and blending). Magnetic agitation simplifies the procedure by agitating cellulose in solution to promote its surface area. Milling enhances the interaction between fibers and the acidic solution by processing the cellulose fibers. Grinding cellulose by a colloidal mill is a process allowing, by varying the intensity of the grinding, to produce the desired fiber size reductions and surface areas.

Mechanical pretreatment affects the final characteristics of CNCs. These are the crystallinity index, total mass yield and particle size distribution. Crystallinity index determines CNC stability and properties. Total mass yield reflects how much CNC is made by individual pretreatments. Particle size distribution is also dependent on pretreatment method. Mechanical pretreatments can decrease production costs due to ability for large-scale production and comparison with intensive approaches. Alternative simpler approaches, like magnetic agitation or homogenization, are able to generate CNC with acceptable properties. Additional studies are needed on the investigation of more severe mechanical pretreatment that may help decrease the hydrolysis time, temperature, or acid concentration. Mechanical pretreatments are critical for CNC production, as they control hydrolysis and modify cellulose properties to allow efficient and low-cost production processes [49].

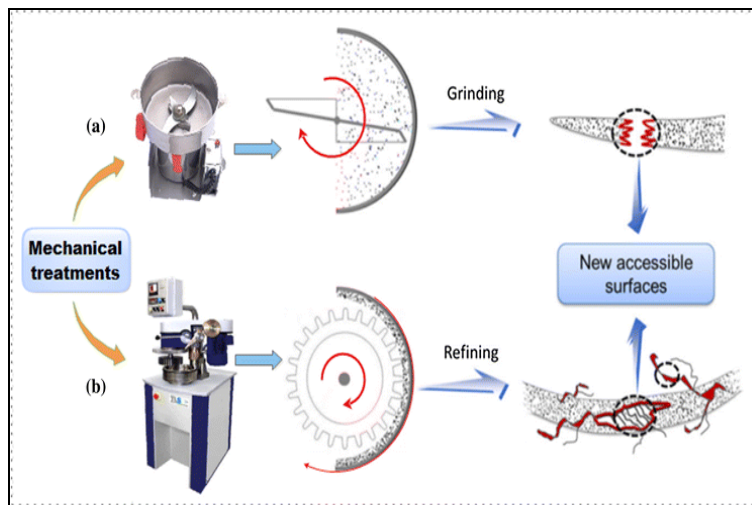


**Fig.1.17: Mechanical treatment of cellulose [50]**

## 1.7 PRETREATMENTS FOR THE EXTRACTION OF NANOCELLULOSE

Lignocellulosic biomass can be converted into cellulose is carried out using several pre-treatments. Breakdown of cell walls and internal tissues of the lignocellulosic biomass can be carried out using pre-treatments as shown in Fig.1.18. The pretreatments can be divided into three types:

- i. Physical pre-treatments: Physical pre-treatments for cellulose extraction includes sonication, pyrolysis, mechanical etc.
- ii. Biological pre-treatments: Non-cellulosic components like lignin and hemicellulose can be removed by biological pretreatments like enzymatic hydrolysis, bacterial treatment etc.
- iii. Chemical pre-treatments: Cellulose can be extracted from raw material using two important chemical pre-treatments which are alkali pulping and bleaching. It helps in removing non-cellulosic

components like pectin, lignin, hemicellulose etc., which are present along with cellulose [51].

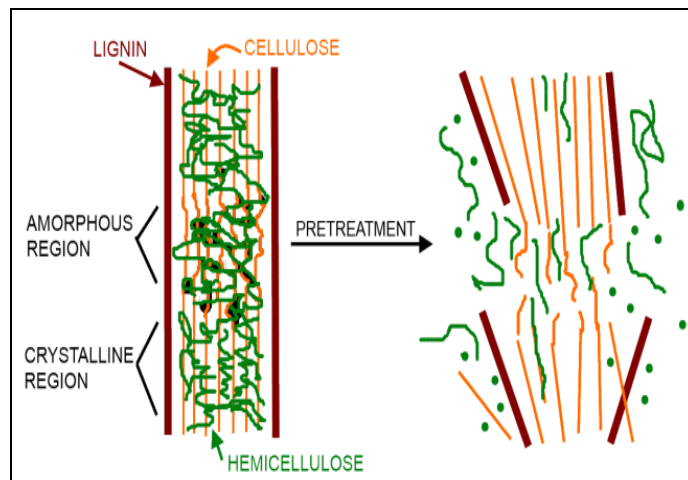


**Fig.1.18: Effect of Pre-treatments [52]**

### 1.7.1 Alkali Pulping

Alkali pulping dissolves and disintegrates non-cellulosic components by encroaching into the crystallites to devastate the inter and intra molecular hydrogen bonds in the cellulose molecules and the nearby crystalline area. The non-cellulosic component hemicellulose is an amorphous entity and it is less densely packed when compared to the crystalline region. So the removal of such amorphous entities increases the degree of crystallinity and the crystallinity index. In most cases sodium hydroxide is used to impregnate the fiber matrix during the alkali pulping process. This process causes the solvation and depolymerization of lignocellulosic materials by breaking the hydrogen bonds that keep cellulose macromolecules together and in combination with other constituents [51].

### **1.7.2 Bleaching**

Bleaching is carried out in the alkali treated sample to remove the non-cellulosic component lignin. Delignification is performed to increase the wettability between the polymer matrix and the natural fiber. Important bleaching agents are hydrogen peroxide ( $H_2O_2$ ), sodium chlorite ( $NaClO_2$ ), sodium hypochlorite ( $NaClO$ ) etc. Due to the presence of lignin, the alkali pulped sample appears to be brown in colour. After bleaching, the cellulose appears to be white in colour whereas the bleaching solution appears to be bright yellow colour [51]. Nagarajan et al. [53] carried out bleaching using 0.7 – 2 wt% of sodium chlorite as bleaching agent and acetic acid ( $CH_3COOH$ ) as buffer solution. Mueller et.al [54] used  $H_2O_2$  (1.3% w/w) and acetic acid (0.1% v/v) for bleaching the alkali pulped sample.

## **1.8 ACID HYDROLYSIS**

The distortions in the amorphous structure makes it more prone to acid hydrolysis when compared to crystalline region. The temperature of the reaction, concentration and type of acid used etc., are the important parameters that influence acid hydrolysis [51]. Fig.1.19 shows the schematic diagram for the isolation of cellulose nanocrystals from waste biomass. There are two types of acid hydrolysis:

### **1.8.1 Mineral Acid Hydrolysis**

Sulphuric acid, hydrochloric acid etc. are the important mineral acids used for acid hydrolysis. It is used for the isolation of nanocellulose from cellulose. Small size, high crystallinity, high thermal stability etc. makes it stand apart. Sulphuric acid is commonly used for acid hydrolysis [51].

Morán et al. [55] used sulphuric acid to isolate nanocellulose from sisal fibres. Camarero Espinosa et al. [56] used phosphoric acid to isolate nanocellulose from cotton pulp.

### 1.8.2 Organic Acid Hydrolysis

Use of organic acid in hydrolysis render less toxicity, high thermal stability, high crystallinity etc.[51]. Sun et al. [57] carried out the hydrolysis of cellulose using 78.22 wt% of formic acid, 17.78 wt% of water and 4 wt% of hydrochloric acid. Mosier et al. [58] carried out acid hydrolysis using 200 mL of 50 mM of maleic acid and sulphuric acid for hydrolyzing cellobiose and microcrystalline cellulose (Avicel).

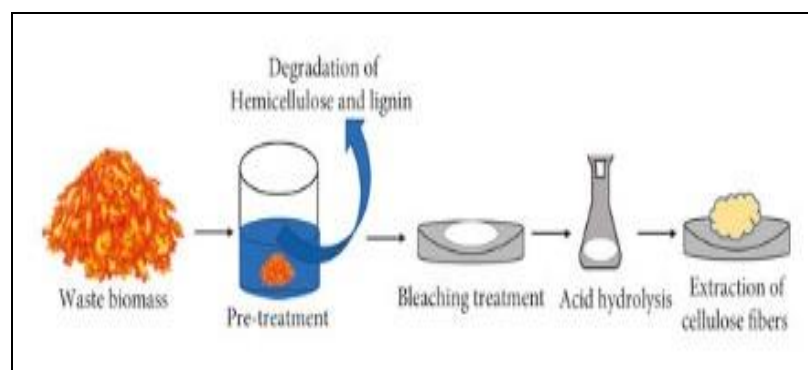


**Fig.1.19: Isolation of Cellulose nanocrystals (CNC) from waste biomass [59]**

## 1.9 APPLICATIONS OF NANOCELLULOSE

Nanocellulose is typically obtained from waste materials, thereby making it a valuable asset in sustainable waste treatment [34]. Fig.1.20 shows the different applications of nanocellulose.

### **1.9.1 Food Packaging Industry**

Cellulose nanofibres (CNF) exhibit good barrier properties due to its fibril structure. It limits the intrusion as well as dispersion of liquid and gaseous materials into cellulose-derived composite films improving the barrier properties of nanocellulose [34]. Not only oxygen barrier properties, but also water vapour barrier properties of bio-based food packaging materials are enhanced by the inclusion of cellulose nanocrystals (CNC) [60].

### **1.9.2 Biomedical Applications**

Nanocellulose is used as a matrix for synthesizing metal nanoparticles like gold [61], silver [62], platinum [63], palladium [64] nanoparticles etc. exhibit efficient antimicrobial activity. Hydrogels based on nanocellulose can be used as drug carriers [34], [65]. Membranes made of nanocellulose are used for wound-dressing. The cellulose nanocrystals can be bestowed with sensing properties by incorporating sensing nanomaterials into the hydroxyl groups present on the surface of cellulose nanocrystals (CNC). This highlights their potential to be used as biosensors [60], [66].

### **1.9.3 Reinforcement in Polymer Matrix**

The incorporation of fillers into polymer matrix composites reinforce their thermal as well as mechanical properties. In today's context attempts are made to replace where non-biodegradable artificial fillers with biodegradable natural fillers to achieve sustainable development and the current focus is on cellulose, chitin, starch etc. Cellulose in nano dimension has enhanced properties when compared to cellulose which include elevated thermal, mechanical and augmented hydrogen bonding which makes it ideal to use as a filler in polymer matrix [34], [67], [68].

The dispersion of cellulose nanocrystals (CNC) in polylactic acid (PLA) matrix can be increased by adding polyvinyl alcohol (PVA) as a surfactant [60].

#### **1.9.4 Water Purification**

The nanocellulose membranes are highly selective. It is coupled with filters and is used to remove harmful contaminants from drinking water like pesticides, dyes etc. Ionic surface active groups like anionic and cationic groups as well as non-ionic surface active groups present in nanocellulose are employed to adsorb and remove natural as well as heavy metal impurities from aqueous solutions [34].

#### **1.9.5 Papermaking Industry**

High crystallinity, high surface area, increased amount of hydrogen bonds etc. makes cellulose nanocrystals a promising factor in papermaking industry. But they also have water retention properties restraining its potential as paper coating materials [60]. Inclusion of electro-conductive fillers like carbon nanotubes (CNT) can be leveraged to produce electro-conductive cellulosic papers [60], [69].

#### **1.9.6 Food Additives**

Cellulose can be used as an emulsifier, stabilizer, thickener etc. because it doesn't affect the food quality. Cellulose nanocrystals (CNC) forms "Pickering emulsions" because the solid particles aggregate at the oil-water interface. Therefore, it can be used as stabilizers [60].

### 1.9.7 Catalysis

Cellulose nanocrystals (CNC) have high surface area and plenty of electron-rich hydroxyl groups [60]. So they can be used in many sustainable applications like cellulose nanocrystals supported palladium where it can be used as a recyclable catalyst [70], fabrication of cellulose nanocrystals (CNC) supported stable Fe (0) nanoparticles [71] etc.

### 1.9.8 Carbon Dots

C-dots were made from CNCs, which are a good source of carbon. Nitro-substituted C-dots are obtained more easily when hydrolyzed sugar moieties on the surface of CNCs react with nitrogen sources. This dual role improves synthesis efficiency. By combining carbon dots with CNC, its optical properties can be enhanced.

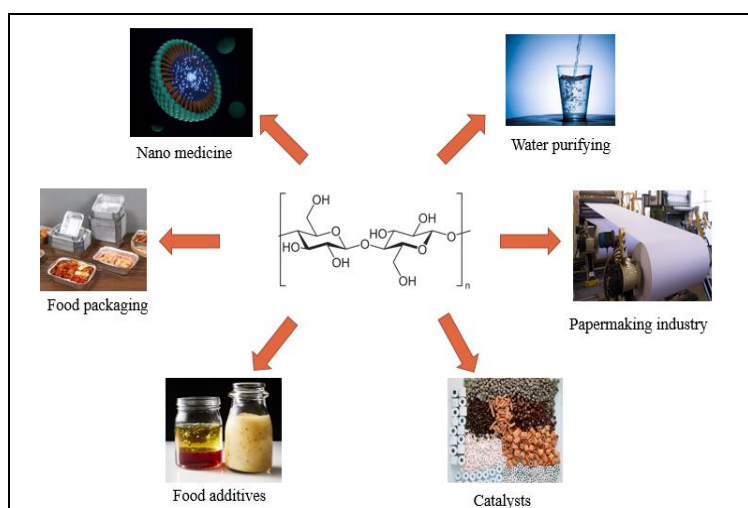


**Fig.1.20: Applications of Nanocellulose**

## **1.10 CHITIN AND CHITOSAN**

Chitin is a naturally occurring mucopolysaccharide that is white, hard, inelastic, and nitrogenous. It is a byproduct of the sea food industry. It is recognized as a regenerating raw resource that is only second in amount to cellulose. Chitin and chitosan are versatile and promising biomaterials. Chitosan, a de-acetylated chitin derivative, is a more practical and intriguing bioactive polymer. Every year, about a thousand tonnes are produced naturally, with marine species accounting for over 70% of the total percentage. Chitin is the principal substance found in the shells of crustaceans such as prawns, crab, and lobster. It is also found in the cell walls of various fungi, as well as the exoskeletons of mollusks and insects. Chitosan is mostly manufactured by Deacetylation or removal of acetyl groups from the chitin polymer by alkali treatment is done commercially (Fig.1.21 (b)).

Chitin's major component is (1-4)-linked 2-acetamido-2-deoxy-D-glucosamine (N-acetylglucosamine) (Fig.1.21 (a)). Despite the fact that it does not exist in cellulose-producing organisms, it is commonly recognized as a cellulose-polysaccharides. Amount of N- acetylglucosamine and glucosamine is determined by degree of deacetylation. Despite being biodegradable, it has a large number of reactive amino side groups, which opens the door to a wide range of useful derivatives that are either commercially available or can be produced by graft reactions and ionic interactions. India, Poland, Japan, the United States, Norway, and Australia are currently commercial producers of chitin and chitosan. A substantial amount of research is being conducted on chitin/chitosan around the world, particularly in India, to explicitly impart the competencies required to maximize its value.

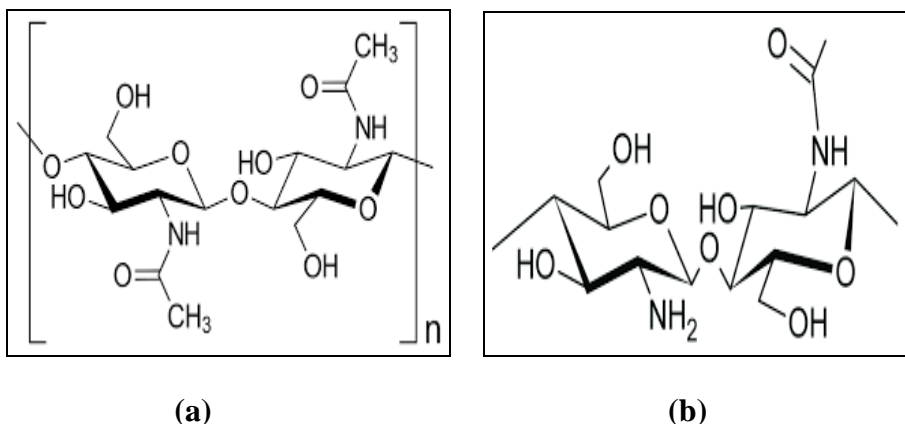


Fig.1.21 Structures of (a) Chitin (b) Chitosan

Because of its fundamental characteristics - such as its muco adhesiveness, non-toxicity, and biodegradability - chitosan is highly sought-after in a wide range of applications, including biomedicine, pharmacy, biotechnology, the food industry, and nanotechnology [72], [73].

### 1.10.1 Properties of Chitosan

The primary characteristics of chitosan are its molecular weight (MW) and degree of acetylation (DDA). The number of free amino groups in the structure is impacted by deacetylation, which is the removal of acetyl groups from chitin and their replacement with reactive amino groups (NH<sub>2</sub>). Since DDA affects both the physicochemical and biological properties of chitosan, it is seen to be an essential feature. These parameters significantly affect the functional properties of chitosan, such as its solubility, material-forming capacity, biodegradability, and range of bioactive properties. Greater degrees of deacetylation (DDA) chitosan films showed reduced swelling indices, greater elastic modulus and tensile strength, and enhance crystallinity compared to lower DDA films. Chitosan's reactive amino and hydroxyl groups enable it to attach to metal ions and form complexes. Safe, non-toxic, biocompatible, hemostatic, fungistatic, spermicidal, anti-tumor,

anti-cholesteric, and strongly binding to both mammalian and microbial cells are some of its biological characteristics [72], [73].

### **1.10.2 Applications of Chitosan**

The usage of chitosan in various biopharmaceutical research fields, including muco adhesion, permeation enhancement, vaccine technology, gene therapy, and wound healing and it recently employed in mucosal vaccination and gene delivery, as well as ocular, nasal, sublingual, buccal, periodontal, gastrointestinal, colon-specific, vaginal, and transdermal medication delivery. Chitosan is also used as food packaging due to its nontoxicity, antimicrobial, bactericidal, permeability, and mechanical properties. Chitosan is used in bioremediation because it is a natural active absorbent that can be used to absorb heavy metal ions. It is also used in pharmaceutical field to directly compress tablets, act as a tablet disintegrant, create controlled-release solid dosage forms, or enhance drug absorption. It can also be used to coat seeds for fruits, vegetables, nuts, and cereals. It increases proline and sugar contents, thereby changing the seed plasma membrane permeability. It also improves the activity of the enzymes peroxidase, phenylalanine ammonia- lyase, tyrosine ammonia- lyase, and catalase. Chitosan acts as an antifungal, antiviral, and bionematicidal agent. Chitosan acts as a carrier promoting slow- release of fertilizers. It also improves the water retention capacity of the soil. Chitosan also has the best chelating properties, is able to remove heavy metals and dyes, controls algal contamination from lakes, and acts as a soil conditioner. Chitosan shows good film properties. Due to these properties, chitosan is used as polymer matrix for the composite film. Chitosan shows application in numerous field such as tissue engineering, cancer diagnosis,

ophthalmology, anti-thrombogenic and hemostatic materials, anti-aging properties, anti-tumor activity, water engineering, the paper and textile industries, agriculture, photography, etc [72], [73].

## **1.11 QUANTUM DOTS**

Quantum dots are extremely tiny semiconductor particles, usually measuring between one and ten nanometers in diameter. Because of their minute size, quantum dots have special characteristics that result from quantum confinement effects, in which electron and photon behavior is controlled by quantum mechanics instead of classical physics. Quantum dots are extremely sought for a variety of applications in photonics, electronics, and nanotechnology because of their size-dependent behavior, which is essential to their tunable optical and electrical properties. Quantum dots' (QDs') properties fall in between those of bulk semiconductors and discrete atoms or molecules. Their size and shape have an impact on their optoelectronic properties. One of the most important optical properties of colloidal quantum dots is color [74].

### **1.11.1 TYPES OF QUANTUM DOTS**

Quantum dots are commonly categorized based on their elemental constitution as:

- 1. II – VI QUANTUM DOTS**
- 2. III – V QUANTUM DOTS**
- 3. IV – VI QUANTUM DOTS**
- 4. SILICON QUANTUM DOTS**
- 5. GRAPHENE QUANTUM DOTS**
- 6. CARBON QUANTUM DOTS**

### **1.11.2 CARBON QUANTUM DOTS**

Carbon quantum dots, sometimes referred to as C-dots, CDs, or CQDs, are semiconductor nanocrystals that possess a number of unique characteristics. Usually, they are very small carbon nanoparticles. CDs are typically described as quasi-0D carbon-based materials with intrinsic fluorescence that are less than 10 nm. When single-walled carbon nanotubes were being purified, these particles were inadvertently created. They have been employed extensively in a growing variety of industries in recent years. Compared to traditional semiconductor quantum dots and organic dyes, photoluminescent carbon-based quantum dots have better qualities such high solubility, strong chemical inertness, simplicity of modification, and excellent resistance to photobleaching [75].

Compared to other carbon-based nanomaterials, CDs are more cost-efficient, have a larger effective surface area, better charge transferability, higher electroconductivity, and less toxicity. A variety of functional groups, including as amino, carboxyl, and hydroxyl, can be added to the surface of carbon dots to change their characteristics, increase stability, permit particular interactions, and improve biocompatibility. CDs have excellent electrical conductivity when employed as electrocatalysts in electrocatalytic reactions. A variety of functional groups, including as amino, carboxyl, and hydroxyl, can be added to the surface of carbon dots to change their characteristics, increase stability, permit particular interactions, and improve biocompatibility. CDs have excellent electrical conductivity when employed as electrocatalysts in electrocatalytic reactions. Because of their exceptional optical qualities, fluorescent CDs have found extensive usage in a variety of medical applications, especially in the fields of biosensing, bioimaging, and therapeutic development [75].

## **1.12 FLUORESCENT INK**

Fluorescent ink is a particular ink type especially helpful for security features on documents, promotional materials, and other applications where a striking, visible glow under UV light is desired because it contains pigments that can absorb invisible ultraviolet light and re-emit it as visible light, creating a bright, vibrant colour that is only visible when exposed to a UV light source. It includes fluorescent pigments, which absorb ultraviolet light and re-emit it at a longer wavelength as visible light. They are frequently employed in security features such as passports, certificates, banknotes, promotional products, anti-counterfeiting measures, and creative creations where a vivid glow is sought [76], [77], [78].

## **1.13 ANTIOXIDANT ANALYSIS**

Free radicals, also known as ROS, are substances or small particles with unpaired electrons in their atomic or molecular orbitals. They also include a variety of oxygen species, including hydrogen peroxide, a potent oxidizing functional group that cells produce during respiration and cell-mediated immune responses. Free radicals are given electrons by antioxidants, which neutralize them and make them appear innocuous, reducing oxidative damage to biological processes. Oxidative stress is the main factor linked to free radicals. Oxygen reacts with certain chemicals to produce free radicals, which can then interact with vital biological components like proteins and DNA to cause harm as well as damage to the cell membrane. By reacting with free radicals, antioxidants can neutralize them and prevent harm before it begins. Among the many different types of secondary metabolites that plants produce are antioxidants. A

interaction with an antioxidant can produce a stable DPPH-H (2, 2-diphenyl-1-hydrazine) complex along with a color shift from purple to bright yellow. DPPH (2, 2-diphenyl-1-picrylhydrazyl) radicals are stable free radicals because a single pair of electrons on the N atom is surrounded by three benzene rings. The outcome showed that CDs did have scavenging activity against DPPH. It is possible for carbon dots to scavenge free radicals. Additionally, it has been demonstrated that when exposed to visible and/or ultraviolet light, some forms of C-dots act as oxidizing agents. Particularly fascinating is this dual oxidant-antioxidant nature, which is intimately associated with the C-dot characteristics [79], [80].

### **1.14 OBJECTIVES**

- Extraction of cellulose and removal of non-cellulosic components from jackfruit peels through alkali treatment and bleaching.
- Synthesis of cellulose nanocrystals from cellulose using hydrothermal assisted oxalic acid hydrolysis.
- Characterization of raw material, cellulose, and cellulose nanocrystals (CNC) using FTIR, XRD, TGA, FESEM and TEM to confirm the successful extraction and evaluate the properties.
- Synthesis of carbon quantum dots using cellulose.
- Characterization of carbon quantum dots using UV- Visible and PL spectroscopy.
- Analysing the anti-oxidant activity of the synthesized carbon quantum dots.
- Formulation of fluorescent ink using the synthesized carbon quantum dots.

- Extraction of chitin from shrimp shell waste and synthesis of chitosan from chitin.
- Studies of moisture and ash content of chitin and chitosan, viscosity and Degree of Deacetylation (DDA) of chitosan.
- Fabrication of eco-friendly bio-nanocomposite films using a PVA/Chitosan matrix reinforced with cellulose nanocrystals (CNCs) via solution casting.
- Characterization of PVA/Chitosan and PVA/Chitosan/CNC nanocomposite films using FTIR, FESEM and measuring its tensile strength to evaluate its composition and strength.
- Examining the oil absorption capabilities of PVA/Chitosan/Cellulose nanocrystals (1% CNC) nanocomposite films in petrol-water mixture, thereby evaluating its potential as an eco-friendly solution in oil spill remediation.
- Development of printable cellulose paper from jackfruit peels as a sustainable alternative to traditional paper.

# Chapter 2

## LITERATURE SURVEY

Hu et al., (2014) reported the preparation of carboxylated cellulose nanocrystals (CCN) and cellulose nanocrystals (CNC) from the borer powder of bamboo. Two steps were adopted for the preparation. One-step approach with ammonium persulfate for the preparation of carboxylated cellulose nanocrystals (CCN) and two-step approach with sulfuric acid for the preparation of cellulose nanocrystals (CNC). The synthesized samples were characterized using transmission electron microscopy (TEM), Fourier transform infrared spectroscopy (FTIR), X-ray diffraction (XRD) and thermogravimetric analysis (TGA). Morphology studies reveal that the particles of carboxylated cellulose nanocrystals (CCN) and cellulose nanocrystals (CNC) are spherical in shape having diameters in the range 20-50 nm and 20-70 nm respectively. After several chemical treatments, the crystallinity of carboxylated cellulose nanocrystals (CCN) and cellulose nanocrystals (CNC) also increased up to 62.75 and 69.84% respectively. This research concludes that the borer powder from bamboo stands out as a promising choice for the synthesis of carboxylated cellulose nanocrystals (CCN) and cellulose nanocrystals (CNC), which in turn is economical and sustainable. It can be further used for the preparation of many other biodegradable products, offering tremendous opportunities in various industries [81].

Sun et al., (2005) focusses on the isolation of cellulose from wheat straw. It involves a two-step process which includes a steam explosion pre-

treatment and alkaline peroxide post-treatment. Initially the straw was steamed at 200°C, 15 bar for 10 and 33 min, and 220°C, 22 bar for 3, 5 and 8 min with a solid to liquid ratio of 2:1 (w/w) and 220°C, 22 bar for 5 min with a solid to liquid ratio of 10:1, respectively. A solution rich in hemicelluloses – derived mono- and oligosaccharides was obtained by washing the steamed straw and which yields 61.3%, 60.2%, 66.2%, 63.1%, 60.3% and 61.3% of the straw residue, respectively. The resulting sample was delignified and bleached with 2% H<sub>2</sub>O<sub>2</sub> at 50°C for 5hrs under pH 11.5, which gave 34.9%, 32.6%, 40.0%, 36.9%, 30.9% and 36.1% (% dry wheat straw) of the cellulose preparation, respectively. The steam explosion pre-treatment performed at 220°C, 22 bar for 3 min with a solid to liquid ratio of 2:1, in which the cellulose fraction obtained had a viscosity average degree of polymerization of 587 and contained 14.6% hemicelluloses and 1.2% klason lignin gave the optimum cellulose yield of 40.0%. The steam explosion pre-treatment led to the removal of hemicellulose and the alkaline peroxide post-treatment led to the elimination of lignin and it increased the crystallinity of cellulose. The resulting six isolated cellulose samples were characterized using Fourier transform infrared spectroscopy (FTIR) and <sup>13</sup>C CP/MAS NMR spectroscopy and thermal analysis [82].

Seta et al., (2020) aims to enhance the output and the colloidal stability of cellulose nanocrystals (CNC) resulting from the hydrolysis of maleic acid. This work is an initiative to synthesize cellulose nanocrystals (CNC) with a high yield and appreciable colloidal stability from bamboo fibres. These bamboo fibres were subjected to ball mill pre-treatment which can disrupt and open up the structure of bamboo fibres, thereby increasing the exposure of hydroxyl groups on the surface of pulp fibres, which in turn

facilitates the penetration of acid molecules into the pulp fibres. Cellulose is easily hydrolyzed by maleic acid, thereby increasing the crystallinity. The maleic acid anhydride reacts with the hydroxyl groups, thereby producing more  $-COOH$  groups on the cellulose nanocrystals (CNC). The resultant cellulose nanocrystals (CNC) showed an increased yield of 10.55-24.50%, which is 2.80% higher than the control. The synthesized cellulose nanocrystals were characterized using Fourier transform infrared spectroscopy (FTIR), scanning electron microscopy (SEM), atomic force microscopy (AFM) and thermogravimetric analysis (TGA). The crystallinity indices were also calculated using Segal's method. Therefore this study provides a convenient method for the synthesis of cellulose nanocrystals (CNC) with high yield and colloidal stability from bamboo fibres, boosting the industrialization of cellulose nanocrystals (CNC) synthesis [83].

Yeganeh et al., (2017) investigates the dependence of the yield, morphology, size and crystallinity of the synthesized cellulose nanocrystals (CNC) on the type of acid and the conditions of hydrolysis. This study intends to synthesize cellulose from the waste office paper. The resulting cellulose was hydrolyzed separately under the same conditions as Maleic acid (MA) and Sulfuric acid (SA). It was also hydrolyzed under different timing and temperature by maleic acid (MA) and sulfuric acid (SA). The synthesized cellulose nanocrystals (CNC) were characterized using X-ray diffraction (XRD), scanning electron microscopy (SEM) and transmission electron microscopy (TEM). The crystallinity index was calculated using Segal's equation which revealed that the resulting cellulose nanocrystals (CNC) are different in their morphology, size, yields and crystallinity under same conditions of maleic acid (MA) and

sulfuric acid (SA). Analysis of the results showed that the cellulose nanocrystals (CNC) prepared using maleic acid (MA) had dominant properties like high yield, high crystallinity and small particle size when compared to the cellulose nanocrystals (CNC) prepared using sulfuric acid (SA). This shows the dependence of the properties of cellulose nanocrystals (CNC) on the type of acid selected for hydrolysis and the conditions of hydrolysis [84].

Rashid & Dutta, (2020) isolated nanocellulose from the husks of short, medium and large rice grains. This study was based on the hypothesis that the nano-scale structural differences would influence the structural differences in the plant parts of the same origin. The delignification and subsequent acid hydrolysis led to the successful elimination of non-cellulosic components, which is confirmed by the increased crystallinity and infrared diffraction. Characterizations like scanning electron microscopy (SEM), transmission electron microscopy (TEM), atomic force microscopy (AFM), zeta potential, X-ray diffraction, thermogravimetric analysis and differential scanning calorimetry (DSC) were carried out. Scanning electron microscopy (SEM) analysis revealed that the compact blocklets having different sizes were formed from the cellulose fibrils of the three different rice husks. Transmission electron microscopy (TEM) and atomic force microscopy (AFM) revealed that smooth surfaced cellulose nanowhiskers released as a result of hydrolysis. They exhibited different sizes like lengths = 55.7–178.6 nm, 111.2–476.7 nm, and 153.1–778.9 nm; diameters = 11.7–28.9 nm, 16.1–37.5 nm, and 19.9–48.3 nm) and aspect ratios (6.4, 9.8, and 16.9). Zeta potential was found to be -33.8 mV, -27.1 mV and -21.3 mV respectively and the crystallinity index was calculated to be 58.82%, 62.32%, and 76.69%. The

cellulose – I allomorphism characterized with XRD peaks at  $2\theta = 16.3^\circ$ ,  $22.4^\circ$ , and  $34.5^\circ$  was retained during the extraction process. Nanocellulose exhibited greater resistance to heat than cellulose and husks. Instead of the two step decomposition pattern observed in the TGA curve for the husk and cellulose, a three step decomposition pattern was observed for nanocellulose due to the extended retention of low molecular weight carbonic residues. Among the small, medium and long rice husks, the long husk was superior in size, crystallinity, strength and thermal stability, followed by medium and then the short husk. The nanocellulose samples showed negligible toxicity (< 0.1% hemolysis) against goat blood erythrocytes. This study also suggests that the synthesized nanocellulose has potential applications as heat resistant materials, food, cosmetic and pharmaceutical industries [85].

Chen et al., (2017) used a novel one-pot oxidative hydrolysis technique to isolate nanocellulose from *Elaeis guineensis* empty fruit bunch biomass. The resulting nanocellulose has physicochemical properties that can be compared with those obtained via traditional multistep purification process such as dewaxing, chlorite bleaching, alkalization and acid hydrolysis. Analysis of the chemical composition of the final product revealed that the cellulose was extracted in major amount (91.0%) with the remaining amounts in minor quantities of lignin and hemicellulose (~6%). High crystallinity was observed for the nanocellulose prepared using one-pot oxidative technique (80.3%) when compared to the nanocellulose prepared using traditional multistep process (75.4%), suggesting that the amorphous regions in the cellulose fibres were removed effectively. Morphology studies revealed that the synthesized nanocellulose exhibited a spider-web like network nanostructure with fibres having an average

diameter of  $51.6 \pm 15.4$  nm. The synthesized nanocellulose exhibited a high thermal stability of  $320^{\circ}\text{C}$  making it suitable to choose for nanocomposite applications. The one-pot oxidative hydrolysis technique serves as a straightforward, flexible and efficient approach for the synthesis of nanocellulose from a complex biomass in just 6 hrs at  $90^{\circ}\text{C}$ , generating less wastewater when compared to traditional multistep processes [86].

Rampazzo et al., (2017) examines the potential oxygen barrier properties of cellulose nanocrystals (CNC) to use it as an oxygen barrier coating on food packaging films. Cellulose nanocrystals possess distinctive properties like biodegradability, renewability etc. This paper deals with the feasibility of producing high performance cellulose nanocrystals (CNC) from reasonable lignocellulosic waste materials. A comparative study was carried out about the cellulose nanocrystals (CNC) obtained through the ammonium persulfate (APS) process of cotton linters and kraft pulp. The poly(ethylene terephthalate) (PET) coated films were analyzed to study its functional properties, as well as the the morphology , chemical properties of the synthesized cellulose nanocrystals (CNC). The results showed that the cellulose nanocrystals (CNC) prepared from cotton linters and kraft pulp exhibited similar characteristics and performances. Also, the coatings made with the cellulose nanocrystals (CNC) prepared from kraft pulp showed excellent gas barrier properties, with the oxygen and carbon dioxide permeability values hundreds of times lower than that of common barrier synthetic polymers of the same thickness, across a wide range of temperatures. These results are relevant in today's scenario to meet the urgent needs paper and plastic industries while contributing towards sustainable development [87].

Li et al., (2013) illustrates the layer-by-layer assembly of two biopolymers, namely chitosan (CS) and cellulose nanocrystals (CNC) on an amorphous PET substrate to study the nanocomposite's oxygen-barrier properties. The oxygen permeability, morphology, and thickness of the nanocomposites were examined under two different pH combinations and with varying deposition cycles, up to 30 bilayers. Each deposited bilayer exhibited a thickness of 7-26 nm, which in turn was highly influenced by the pH value of the solution. The growth process was stable and replicable and the increase in thickness was proportional to the number of bilayers deposited. The combination of chitosan (CS) at pH 4 and cellulose nanocrystals (CNC) at pH 2 showed favourable properties like oxygen barrier properties and better transparency when compared to other pH combinations. The oxygen permeability coefficient of chitosan (CS)/cellulose nanocrystals (CNS) nanocomposites is  $0.043 \text{ cm}^3 \mu \text{mm}^{-2} 24\text{h}^{-1} \text{kPa}^{-1}$  under dry conditions. Both cellulose nanocrystals (CNC) and chitosan (CS) require less energy for their production. The oxygen transmission rate (OTR) measurements reveal that the nanocomposites coatings exhibited good barrier properties, even though the hydrophilic nature of biopolymers used might inversely affect the performance of the film. It concludes with the potential of the chitosan (CS)/cellulose nanocrystals (CNC) nanocomposites in the packaging of food and drug, serving as a clear coating on plastic films and three-dimensional objects like bottles, boxes etc., enhancing both performance and sustainability of the final packages [88].

Azizi et al., (2014) outlines the effect of the addition of cellulose nanocrystals (CNC) on the mechanical, thermal and barrier properties of polyvinyl alcohol/chitosan ((PVA/CS films) nanocomposites films

prepared through the solvent casting process. The synthesized PVA/Chitosan/ Cellulose nanocrystals (CNC) films were characterized using X-ray diffraction (XRD), scanning electron microscopy (SEM), transmission electron microscopy (TEM), thermogravimetric analysis (TGA and DTG), oxygen transmission rate (OTR) and tensile tests were also performed. SEM and TEM studies reveal that the cellulose nanocrystals (CNC) were uniformly distributed in the PVA/Chitosan (CS) matrix at low loading levels. However at higher loadings, agglomeration was observed which adversely effected the film's flexibility and overall performance. When 1.0 wt% of cellulose nanocrystals (CNC) was added to the PVA/Chitosan (CS) matrix, the tensile strength increased from 55.1 MPa to 98.4 MPa and the modulus increased from 395 MPa to 690 MPa respectively. Also, the addition of 1.0 wt% of cellulose nanocrystals (CNC) intensified the thermal stability and oxygen barrier properties of the PVA/Chitosan (CS) matrix. The oxygen transmission rate (OTR) of the nanocomposites films decreased with the incorporation of cellulose nanocrystals (CNC), which in turn increases their barrier properties. So it can be used in applications that require materials with low permeability to gases. The incorporation of cellulose nanocrystals (CNC) into the PVA/Chitosan (CS) blend enhanced its properties, making them suitable for numerous applications like packaging films, drug delivery etc. The biocompatibility and antimicrobial properties of chitosan can be combined with the thermal and mechanical strength of cellulose nanocrystals (CNC), making them a prominent for biomedical applications like wound dressing. They also show potential applications as coatings and adhesives, owing to their biodegradability. By optimizing the formulation, it is able to create high performance nanocomposites films which meets the needs for sustainable development. The increase in demand for renewable and

eco-friendly materials requisites the preparation of such biodegradable films and it plays a crucial role in shaping the future of material science [89].

Perumal et al., (2018) successfully improved essential environmental bio-nanocomposite films by using chitosan (CS) and polyvinyl alcohol reinforced with rice straw derived cellulose nanocrystals (CNC) through acid hydrolysis. The properties of the bio-nanocomposite films were significantly affected by the incorporation of relatively small size (about 15 nm) and rod-like structure of the CNC particles into the PVA/CS matrix, which consequently resulted in the enhancement of the mechanical and thermal properties of the films. The films became better in terms of tensile strength and thermal stability, and at the same time, the level of their crystallinity was also risen without diminishing the transparency, which was an indicator of a good dispersion at the nanoscale. Interestingly, these bio-nanocomposite films are powerful antibacterial and antifungal agents, making them a viable option for food packaging applications. The fact that desolation from rice straw, a waste material from agriculture that would have gone to landfills, can be used to produce the bio-polymer bio-nanocomposite PVA/CS films is something that provides both enhanced performance for the films and sustainability enhancement by waste recycling. The results of this study with the usage of PVA/CS/CNC bio-nanocomposite films for food packaging demonstrate the potential of these films as an eco-friendly and promising alternative that is quite practical and promotes environmental care [90].

Koymeth et al., (2023) presents the development of a novel nanocomposite, consisting of chitosan-garlic peel cellulose nanofibers-

nanocurcumin, which prolongs the storage time of bananas by 8 days. The coating possesses a remarkable antimicrobial activity which is mostly directed against *E. coli*, which also helps to retain the physiochemical trait of the bananas, mitigate weight loss, and restrict the bananas from over-ripening. This is a novel approach as it also addresses the focus of preventing food wastage since the strategy is to utilize biodegradable wastes for production. The study highlights the oxygen barrier effect and antibacterial properties of the coating, which reduce respiration and transpiration rates, thereby enhancing fruit quality. This biobased coating offers a practical and eco-friendly solution for reducing postharvest losses and combating global food waste [91].

Han Lyn & Nur Hanani, (2020) extends his research into chitosan films containing lemongrass essential oil –pointed out them as potential biocomposite materials to be used as food packaging for its antimicrobial properties. The increase in lemongrass essential oil concentration resulted in the improved films elasticity and reduced water vapor permeability, though it somewhat decreased the tensile strength of the modified films due to changes in the microstructure. The films were found to be effective in terms of the anti-microbial activity against foodborne bacteria with some of the strains showing predisposition. The LEO also exhibited some form of volatility that contributed to the anti-microbial activity woody. This was chitosan/LEO films would have the capability of improving food protection during storage and increase their durability. Thus, they raise the necessity for investigating their antioxidant properties and packaging application of the material [92].

Recent studies of Neenu et al., (2023) have explored cellulose Nano papers derived from pineapple pomace as a sustainable material for active packaging. Incorporation of cinnamon essential oil (CEO) into these Nano papers has demonstrated enhanced antibacterial activity against *Staphylococcus aureus* and *Escherichia coli*. CEO addition has also improved water barrier properties and reduced oxygen and water vapor permeability. The plasticizing effect of CEO has been shown to increase the flexibility of the Nano papers while slightly reducing their crystallinity and tensile strength. Applications of these Nano papers in packaging have effectively extended the shelf life of coriander leaves, preserving essential nutrients and reducing weight loss. Such advancements highlight the potential of CEO-loaded Nano papers as eco-friendly solutions for sustainable food packaging [93].

The latest research of Jancy et al, (2020) explains the various chemical processes involved in the extraction of cellulose from jackfruit peels to produce cellulose nanoparticles (CNP). First, the inedible components of jackfruit are treated with a 2% NaOH solution for 180 minutes at 50°C in order to get rid of the hemicellulose and lignin. Bleaching with hydrogen peroxide and NaOH is done until the cellulose turns white, representing high purity. In the final process, the nanoparticles are synthesized from cellulose via acid hydrolysis for about 120 minutes under 52% sulfuric acid at 45°C. The purity characteristics of the resulting CNP demonstrate the absence of certain functional groups, which underscore its potential applications in bionanocomposites, particularly in improving the mechanical and thermal properties of biopolymers for food packaging applications [94].

The studies of Fang et al., (2021) pertains to the synthesis of the C-dots as well as the luminescence properties of these kinds of nanocrystals which were synthetized using a single-step hydrothermal process at varying temperatures, such as 160 °C and 200 °C. Attention should be paid to the fact that heteroatom insertions, such as those of oxygen and nitrogen within the carbon framework, dramatically affect C-dots' optical properties. Different types of fluorescence emission properties-discriminated in excitation wavelength-dependent and excitation wavelength-independent types-were found. The results indicate that C-dots synthesized under 200°C conditions (CDs-200) exhibit excitation wavelength-dependent fluorescent emissions due to well-balanced structural defects, whereas those synthesized at 160°C (CDs-160) exhibit excitation wavelength-independent fluorescence largely owing to a higher proportion of C=O defects. The results demonstrated that increasing the synthesis temperature increases the total number of structural defects, in line with greater fluorescence emission in CDs-200 than in CDs-160. Those characterization methods, applied FTIR and XPS, confirmed that the higher density of defects in CDs-200 increases the optical properties. The stability of the CDs-200 against different treatments-and others UV exposure conditions, changes in pH, etc., indicate their potential in real applications. Overall, this work sheds light on how the microstructural features of carbon dots relate to their luminescence properties, thus laying the groundwork for controlled design of effective fluorescent material [95].

# Chapter 3

## MATERIALS AND METHODS

### 3.1 INTRODUCTION

This chapter includes the materials and methods used for the synthesis of Cellulose Nanocrystals (CNC) and Carbon Quantum Dots (CQDs) from jackfruit peels. PVA/Chitosan and PVA/Chitosan/CNC nanocomposite films were also prepared by solution casting method. Preparation of printable cellulose paper as well as the characterization of the Raw Material (Jackfruit peel powder), Cellulose, Cellulose Nanocrystals (CNC), and Carbon Quantum Dots (CQDs). The prepared nanocomposite films were also analyzed.

### 3.2 SYNTHESIS OF CELLULOSE NANOCRYSTALS (CNC) FROM JACKFRUIT PEELS

#### 3.2.1 Chemicals Required

1. 5% Sodium hydroxide (NaOH)
2. 1.4% Sodium chlorite (NaClO<sub>2</sub>)
3. 30% Oxalic acid (H<sub>2</sub>C<sub>2</sub>O<sub>4</sub>)
4. Glacial acetic acid
5. pH 4 buffer tablets

#### 3.2.2 Materials Required

1. Jackfruit peels

### 3.2.3 Apparatus Required

1. Magnetic stirrer
2. Hotplate
3. Mechanical stirrer
4. Hot air oven
5. Autoclave
6. Sonicator

### 3.2.4 Synthesis of Cellulose Nanocrystals (CNC)

Cellulose extraction was conducted by modifying the acid hydrolysis procedure outlined by R. Brahma and S. Ray [5]. The procedure involved a sequential three stage methodology.

- 1) Alkali Pulping
- 2) Bleaching
- 3) Acid Hydrolysis

The jackfruit peels were collected from household to maintain uniformity in the study. Jackfruit peels were washed well with distilled water and sun-dried for 2 days as shown in Fig.3.1 (a). It was then subsequently oven-dried for two days and grounded using grinder to obtain fine jackfruit peels powder as shown in Fig.3.1 (b).



(a)

(b)

**Fig.3.1: (a) Dried Jackfruit Peels (b) Jackfruit Peel Powder.**

### 3.2.4.1 ALKALI PULPING

Dried jackfruit peels powder is subjected to alkali treatment which involves the solvation and decomposition of non-cellulosic component hemi cellulose. When raw material is treated with alkaline NaOH, it results in fiber swelling, increases the surface area and facilitates hydrolysis of cellulose polymer chain. For this 50 g of jackfruit peel powder was treated in an alkaline medium using a 5% NaOH (w/v) solution at 80°C for 4 hours in a temperature controlled mechanical stirrer. The treated residue was then thoroughly washed to obtain neutral pH. It was then dried at 60°C in a hot air oven as shown in Fig.3.2.

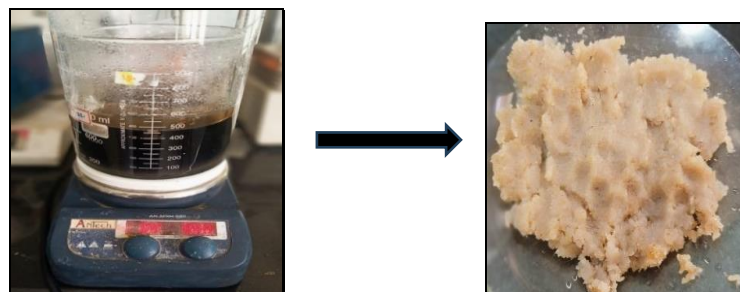


**Fig.3.2: Alkali pulping**

### 3.2.4.2 BLEACHING

The alkali treated fibers were subsequently bleached to remove lignin present in it. Bleaching step also ensure the defibrillation of the cellulose in the material. For this the obtained residue had then undergone bleaching treatment using 1.4% sodium chlorite (w/v) solution at 70°C for 5 hours. It was then followed by washing to achieve neutral pH and dried at 60°C. After bleaching lignin which has brown color gets removed and ensure a

bright yellow bleaching solution. The resulting dried residue constitutes isolated cellulose as shown in Fig.3.3.

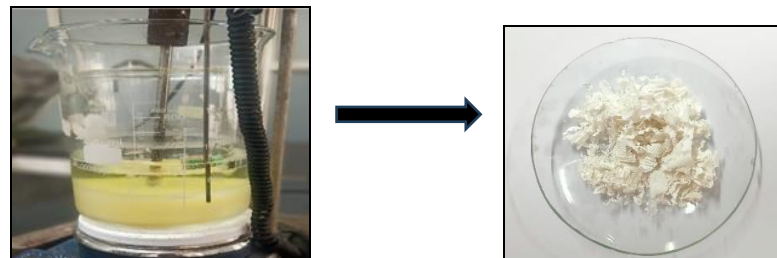


**Fig.3.3: Bleaching**

### 3.2.4.3 ACID HYDROLYSIS

The isolated cellulose was subjected to acid hydrolysis to produce cellulose nanocrystals (CNC) by selective removal of the amorphous region. Cellulose was hydrolyzed with 30% oxalic acid (w/v) solution in a hydrothermal autoclave at 120°C for 6 hours. Oxalic acid which is mild and nontoxic has very less environmental impact compared to other mineral acids. Optimum temperature and pressure were maintained to obtain desired cellulose nanocrystals (CNC). Hydrolyzed residue was washed to neutral followed by sonication for 30 minutes. It was then dried and stored under refrigeration as shown in Fig.3.4.

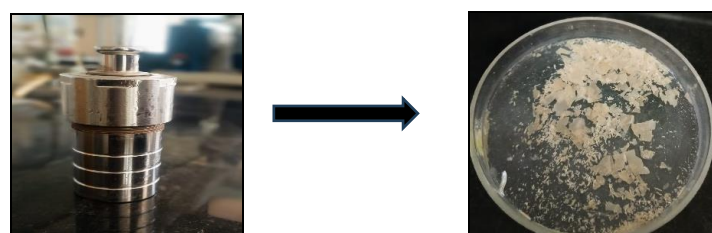


**Fig .3.4: Acid hydrolysis**

Fig. 3.5 Represents the flowchart for the synthesis of cellulose nanocrystals (CNC) from jackfruit peels

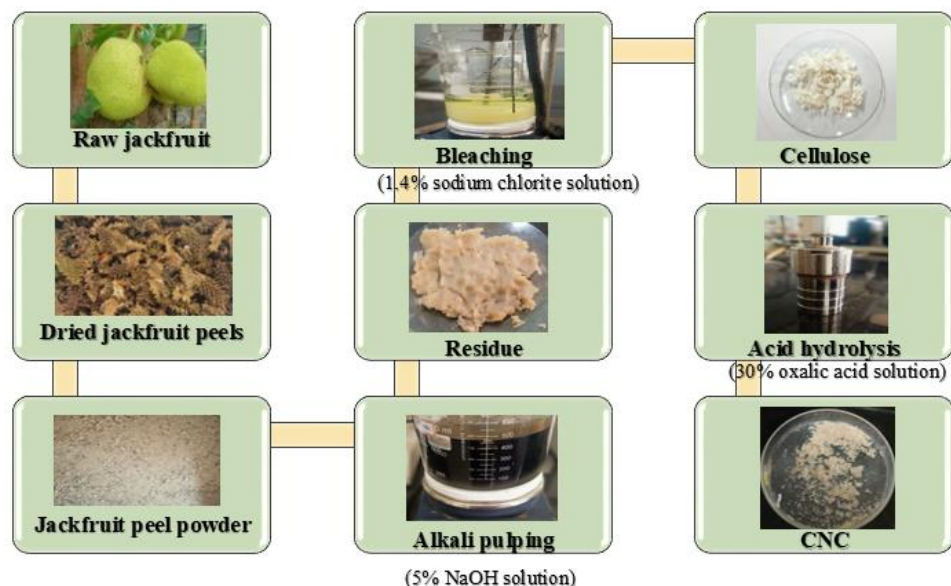


**Fig.3.5: Flow chart showing the synthesis of Cellulose Nanocrystals (CNC).**

### 3.3 EXTRACTION OF CHITOSAN FROM SHRIMP SHELLS

#### 3.3.1 Materials required

1. 1 M NaOH solution
2. Methanol
3. Water
4. Chloroform

### **3.3.2 Extraction of Chitin**

The residual waste from the shrimp shells was gathered, cleaned, dried, and crushed. The powdered shell undergoes deproteinization, an alkali process, for 72 hours at 65–100° C using 1 M NaOH. The second phase is called demineralization. The shell is treated with 0.275–2.0 M HCl for 1–48 hours at 0–100° C following deproteinization. This is followed by decolorization and bleaching using an organic mixture of methanol, water, and chloroform in a 1:2:4 ratio at 25° C.

### **3.3.3 Extraction of Chitosan from Chitin**

- 1.** Chitin
- 2.** 50% NaOH solution
- 3.** Hot air oven

The process of deacetylating chitin yields chitosan. In this process, chitin is treated for 6–8 hours with 50% NaOH (1:10 w/v). After that, the product was filtered and cleaned with distilled water until the pH was balanced. The finished products were dried for a further 24 hours at 40° C in a vacuum oven after first being dried for 24 hours at 40° C in a conventional oven.

## **3.4 DETERMINATION OF ASH AND MOISTURE CONTENT OF CHITIN AND CHITOSAN**

### **3.4.1 Materials required**

- 1.** Chitin or chitosan
- 2.** Dessicator
- 3.** Muffle furnace

**4. Hot air oven**

**5. Petri dish**

Five grams of chitin/chitosan was taken in a petri dish and heated for 5 hours in oven at 105°C. The petri dish was placed in desiccator to cool after the heating phase. The moisture content can be determined by comparing the weight before and after the heating procedure.

To determine the ash content two grams of chitin/chitosan was taken in crucibles and heated in a muffle furnace at 800° C for three hours. After that, it was cooled gradually and weighed to determine the ash content using equation.

$$\text{Ash content (\%)} = \frac{W_1 - W_2}{2} \times 100$$

where  $W_1$  and  $W_2$  are weight before and after heating in muffle furnace.

### **3.5 DETERMINATION OF VISCOSITY AND DEGREE OF DEACETYLATION (DDA) OF CHITOSAN**

#### **3.5.1 Materials required**

- 1. Chitin or chitosan**
- 2. 1% Acetic acid solution**
- 3. Brookfield viscometer**
- 4. Round bottom flask**
- 5. 12N Sulphuric acid**
- 6. 1N Hydrochloric acid**
- 7. 0.1N NaOH**

### **8. Mechanical stirrer**

Three grams of chitosan was dissolved in 300 ml of 1% acetic acid solution and continuously stirred for three hours. It was filtered and a Brookfield viscometer was used to test the viscosity of the filtered solution.

The process for measuring the degree of deacetylation (DDA) involves dissolving one gram of chitosan in 12N sulfuric acid in a round-bottom flask and subjecting it to reflux for thirty minutes. Add 50 ml of distilled water to start the distillation process. Titrate it with a 0.1N NaOH solution. Using the titre values, DDA was determined using equation,

$$DDA = \frac{0.2069 - x}{0.2069} \times 100$$

where,

$$x = \frac{titre\ value \times 42 \times 0.1}{1000}$$

## **3.6 PVA /CHITOSAN/ CNC FILM**

The synthesized cellulose nanocrystals (CNC) were further blended with chitosan and polyvinyl alcohol (PVA) to form composite films with potential applications in dye degradation, biodegradable food packaging and in oil spill remediation.

### **3.6.1 Chemicals required**

1. Poly(vinyl alcohol) (PVA)
2. 1% Acetic acid

**3. Chitosan (CS)**

**3.6.2 Materials required**

1. Lemongrass oil
2. Nano curcumin

**3.6.3 Apparatus required**

1. Petri dish
2. Hot plate
3. Magnetic stirrer
4. Sonicator

**3.6.4 Preparation of PVA/Chitosan/CNC Nanocomposite Film**

To prepare the PVA/Chitosan/CNC nanocomposite film, 1:1 ratio of Polyvinyl Alcohol (PVA) and Chitosan was used, with 0.5 g of each PVA and Chitosan dissolved in hot distilled water and 1% acetic acid solution, respectively. The two solutions were then stirred for 30 minutes for blending. To this 0.01/0.03/0.05g of cellulose nanocrystals (CNC) were gradually added to the PVA/Chitosan mixture and blended for 3 hours to get 1%, 3%, 5% PVA/ Chitosan /CNC nanocomposite films respectively. The final blend was cast into a petri dish and dried at room temperature to form the composite film. A PVA/Chitosan blend film was also prepared following the same process without cellulose nanocrystals (CNC) addition for comparison [96], [97]. Fig.3.6 represents the preparation of PVA/Chitosan/CNC nanocomposite film.

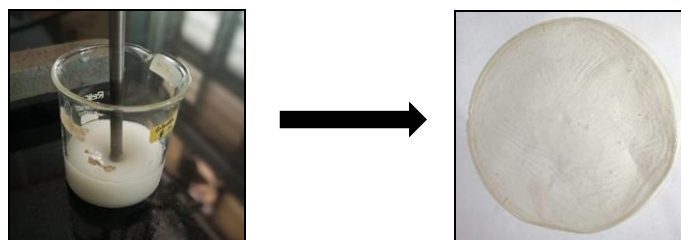


**Fig.3.6: Preparation of PVA/Chitosan/CNC Nanocomposite film**

### 3.7 SYNTHESIS OF CARBON QUANTUM DOTS

Cellulose is an excellent source for synthesis of carbon quantum dots because it's abundant, renewable and eco-friendly. Its natural properties allow for tunable optical features like fluorescence, which can be adjusted by changing synthesis conditions making it a green alternative to traditional carbon-based sources for fabricating CQDs. Additionally, the functional groups on cellulose's surface can be used to modify the carbon quantum dots properties, making it a versatile and sustainable material for nanomaterials.

#### 3.7.1 Hydrothermal Method

Hydrothermal synthesis is a most widely used techniques for developing carbon quantum dots (CQDs) from cellulose, which mainly vary in the use of solvent and reaction conditions. Hydrothermal synthesis uses water as the medium, high temperature and high pressure (120–280 °C), closed system, where cellulose or derivatives thereof carbonize, nucleate and yield carbon quantum dots. This approach is environmental friendly, economical, and easy to implement which makes it popular for cellulose-based CQDs.

### **3.8 ANTIOXIDANT ANALYSIS**

A mixture of 1.5 mL sample and 1.5 mL 0.2 mM ethanolic DPPH solution was vortexed and incubated in darkness for 30 minutes. The absorbance was measured at 517 nm with ethanol as the blank and DPPH solution without the sample as the control. The sample with lower absorbance expresses a more significant free radical scavenging activity (RSA) [79], [80].

### **3.9 CARBON QUANTUM DOT BASED FLUORESCENT INK FORMULATION**

An ink pen refill tube was filled with the carbon quantum dot solution without any preprocessing. On filter paper, it was used to write and draw a variety of designs and text. Fluorescent images were created by exposing it to UV light after it had been in the air.

### **3.10 CELLULOSE PAPER**

Cellulose is an important intermediate during the synthesis of cellulose nanocrystals (CNC) from jackfruit peels. They are usually prepared from plant sources, thereby reducing environmental pollution and contribute to sustainable development. The presence of hydroxyl groups in cellulose render them sufficient functionalities. It possess a highly porous structure with a very large surface area. It is biodegradable and biocompatible. Thus we can introduce various polymers as well as functional groups, thereby strengthening its applications. It can be used as filters and electrical insulators in industries. It can be used for writing, printing etc., therefore it finds application in our day-to-day life as well [98].

### **3.10.1 Materials required**

1. Cellulose

### **3.10.2 Apparatus required**

1. Petri dish
2. Hot air oven

### **3.10.3 Preparation of Cellulose Paper**

The cellulose residue derived from jackfruit peels was casted in a petri dish and was oven dried at 60°C for 2 days to obtain a printable cellulose paper. It is an enhanced replacement for convectional paper.

## **3.11 CHARACTERISATION TECHNIQUES**

The raw material (jackfruit peel powder), synthesized cellulose and cellulose nanocrystals (CNCs) were characterized using X-ray diffraction (XRD), Fourier transform infrared spectroscopy (FTIR), Scanning electron microscopy (SEM), Transmission electron microscopy (TEM) and Thermogravimetric analysis (TGA). The prepared PVA/Chitosan film and PVA/Chitosan/CNC nanocomposite films were characterized using Fourier transform infrared spectroscopy (FTIR) and by measuring their tensile strength.

### **3.11.1 X- Ray Diffraction (XRD)**

X-ray diffraction (XRD) is used to analyze crystalline materials. Here, a crystalline material is subjected to monochromatic beam of X-rays. These X-rays on striking with the lattice planes of the crystal gets scattered at different angles which in turn produces different diffraction peaks as a result of constructive interference. Information regarding the atomic

arrangement within the material can be obtained by analyzing these peaks. This X-ray diffraction pattern acts as a “fingerprint” of the material’s periodic atomic rearrangement. Thus we could evaluate the crystalline nature of the analyze sample. Its non-destructive nature sets itself apart from other techniques. It offers rapid and straightforward sample preparation. The d-spacing calculations have high precision and can be conducted in real-time. So we can characterize a wide range of materials using this technique including single crystals and amorphous solids. This technique is optimized for homogenous, single-phase materials. Another disadvantage is that it requires the sample to be in powder form. It also needs to have access into standard reference files. Its effectiveness decreases when it comes to mixed materials, with a detection limit of 2%. Even the overlapping of peaks may occur at higher angles. It finds application in pharmacy, aerospace, mineralogy etc [99].

XRD analysis was performed to identify the crystalline nature using Bruker AXS D8 Advance X-Ray Powder Diffractometer with a Cu K $\alpha$  radiation source having wavelength 1.54  $\text{\AA}$  operating at 35 mV current and 40 kV voltage [95]. Using the Segal equation the crystallinity indices were calculated [101].

$$I_c (\%) = (1 - I_{am} / I_{200}) \times 100\%$$

### **3.11.2 Fourier Transform Infrared Spectroscopy (FTIR)**

FTIR analysis was performed to identify the different functional groups. In FTIR spectroscopy, the amount of infrared radiation absorbed by the sample is measured. Here the different ranges of frequencies emitted by the source are isolated using a grating or a prism. Then, the energy corresponding to each frequency is measured using a detector and an

intensity vs frequency spectrum is plotted. FTIR can be used for both quantitative and qualitative analysis. It is used for structural elucidation and compound identification qualitatively. The amount of material present can be determined by evaluating the size of the peaks. It gained widespread recognition due to its simplicity and clear underlying principle. It is widely used as an analytical technique and it can be subjected to further refinement in future. Even though dispersive instruments use double beam, FTIR's reliance on single beam is a major limitation because it may affect its precision. It shows potential application in diverse fields including nanotechnology, forensic science, pharmacy, food and beverage industry etc. [102]

FTIR analysis was carried out in the raw material, cellulose and CNC to confirm the removal of non-cellulosic contents like hemicellulose and lignin and the successful extraction of CNC from cellulose using Thermo Scientific Nicolet 912A0712 iS5 FT-IR Spectrometer. The spectra were taken in the wavelength range between 4000-400  $\text{cm}^{-1}$  in the mid-IR range and with a resolution of 4  $\text{cm}^{-1}$ . The reading was taken using % transmittance [100].

### 3.11.3 Scanning Electron Microscopy (SEM)

Scanning electron microscopy (SEM) provides information regarding the topography, composition and crystallography of a sample. SEM generate a high resolution image by scanning the surface of a specimen using a focused beam of electrons. It can show magnification from 5x to 300,000x and even up to 1,000,000x in modern equipments. The instrumentation includes electron source, condenser, objective, detector etc. Firstly, the sample is scanned using the electrons and the emitted electrons are detected to generate SEM images. Conventional SEM (CSEM), Low

Voltage SEM (LVSEM), and Environmental SEM (ESEM) are some the examples of different types of SEM. Energy Dispersive X-ray Spectroscopy (EDS) is performed alongside SEM to analyze the surface characteristics of a sample as well as the quantitative and qualitative results. It gives three-dimensional images. It doesn't require ultrathin samples and is also less time consuming when compared to TEM. But scattering of beam can occur when the electron beam reacts with the sample which may adversely affect the resolution of the image. SEM is employed in nanotechnology, biology, material science etc. [103]

To obtain the high resolution images and detailed information of raw material, cellulose and CNC surface, Field Emission Scanning Electron Microscope with EDS (Tescan Brono MA1A3 XMH) was used.

### **3.11.4 Transmission Electron Microscopy (TEM)**

Transmission electron microscopy (TEM) is an important imaging technique for analyzing the morphology of materials and its fine structure. One of the underlying condition for TEM is that the mean free path of the electrons can be optimized by optimizing a high vacuum in the column, thereby proving a clear image of the sample. The transmitted electrons are made to pass through an ultrathin sample usually around 100 nm thick by focusing and magnifying them. This technique outshines itself for its ultrathin resolution. Therefore, objects can be observed in nano dimensions. TEM is used in tandem with energy-dispersive X-ray (EDX) to evaluate the elemental composition of the analyzed sample. Thus we could evaluate the features and attributes of the analyzed samples. Selected Area Electron Diffraction (SAED) is carried out in parallel with TEM to evaluate the crystallography of the analyzed sample. Information regarding the arrangement of atoms in the crystal lattice can be obtained

using TEW with SAED. Both dark-field and bright-field images can be obtained using TEM. Preparation of ultrathin samples renders some difficulty in sample preparation. It causes radiation damage to the samples and requires high vacuum conditions. It has smaller field of view when compared to SEM and it is very expensive. TEM is widely used to characterize electronic devices, metallurgy, biology, nanotechnology etc. [104]

TEM analysis was performed to analyze the morphology of individual nanocrystals dimensions and aspect ratio [53]. It was carried out using High Resolution Transmission Electron Microscope (Jeol JEM 2100).

### **3.11.5 Thermogravimetric (TGA) Analysis**

Thermogravimetric analysis (TGA) evaluates the changes in the mass of a sample as a function of temperature. TGA sheds light on the sample's thermal stability, formulation and degradation pattern. It measure the changes in the weight of a sample when it is exposed to different temperatures and atmospheres. Differential thermal analysis (DTA) detects the change in temperature between the reference material and the sample even though they are exposed to the same amount of heat flow for evaluating thermal phenomena like chemical reaction, phase transformations, melting point etc. It also helps in detecting endothermic and exothermic reactions. Both TGA and DTA can be used together for better characterization of the thermal properties of the analyzed sample. TGA spectrum is plotted with mass against temperature/time and the DTA curves are plotted with differential temperature against time/temperature. They are highly sensitive and can be used to analyze a wide range of materials like metals, biological materials etc. They are also non-

destructive techniques. Both TGA and DTA has some restriction when it comes to the temperature ranges they have access to. There is some complexity in interpreting the data. Also, it requires specificity for the sample sizes and the samples have to be prepared carefully. It finds applications in various fields like pharmacy, quality control etc. [105]

The thermal performance (TGA/DTA up to 750°C) was carried out to determine the rate of change of weight with respect to temperature (°C) in a N<sub>2</sub> atmosphere in a flow rate of 20 mLmin<sup>-1</sup> [10], [11]. The Differential Scanning Calorimetry was performed using Differential Scanning Calorimeter (Mettler Toledo DSC 822e).

### **3.11.6 Mechanical Properties (Tensile strength)**

Mechanical properties refers to the behaviour of a substance under different stress conditions. Strength refers to the material's ability to resist certain load without breaking. It is divided into two: One is tensile strength which is the maximum amount a stress a material can tolerate while being strained and the other one is compressive strength which is the material's ability to tolerate compressive stress. Another property is ductility which is the material's ability to undergo plastic deformation without breaking. Brittleness is the ability of a material to exhibit little to no plastic deformation before rupturing. A material's ability to resist wear and tear is called hardness. Elasticity is the material's ability to regain its size and shape when the external load is removed whereas plasticity is the permanent deformation when the material is exposed to a load exceeding its elastic limit [107].

Tensile strength (TS) and the percentage elongation at break of PVA/CS/CNC films were determined according to the standard methods.

### **3.11.7 UV – Visible Spectroscopy**

UV spectroscopy, or UV-visible spectrophotometry (UV-Vis or UV/Vis), is an analytical technique involving the measurement of absorption or reflection in the ultraviolet and visible regions of the electromagnetic spectrum. Since it works with visible light, it will directly influence the apparent color of materials. The atoms and molecules in this region undergo electronic transitions.

Absorption spectroscopy is complementary to fluorescence spectroscopy, in that molecules with bonding or nonbonding electrons are able to absorb visible or UV light and excite these electrons into higher-energy antibonding molecular orbitals. The ease of excitation controls the wavelength of absorbed light, with easily excited electrons absorbing longer wavelengths.

This technique is widely used in analytical chemistry for the analysis of a variety of analytes like transition metal ions, highly conjugated organic compounds, and biological macromolecules. Transition metal ions, for example, are usually colored due to d-electron transitions, and their color can be altered by interaction with ligands.

The instrumentation used in this technique is a UV-visible spectrophotometer. It measures the transmitted light intensity of a sample ( $I$ ) and compares it with the original intensity before the sample ( $I_0$ ). The percentage transmittance (%T) is denoted by,

$$A = -\log (\%T/100)$$

### **3.11.8 Photoluminescence Spectroscopy**

Photoluminescence spectroscopy is a powerful method of materials characterization, especially which of carbon- based materials such as carbon quantum dots (CQDs). It requires excitation of an example material by photons with a definite wavelength from a lamp or laser light, which transfers the electrons into upper energy states. The emitted electrons when going to the base level emit photons with lower energies, which is known as luminescence.

Photoluminescence spectra give useful information on surface characteristics, quantum efficiency, and emission characteristics of CQDs. The peaks of emission seen in the spectra are due to particular energy transitions in CQDs, enabling one to study changes in surface functionalization, size, and chemical makeup. This method also enables one to assess quantum yield, which gives a measure of light emission efficiency when excited.

Aside from emission efficiency, photoluminescence spectroscopy can be employed to investigate how functional groups and surface states affect CQD properties and evaluate their photostability and stability under varying environmental conditions. Generally, this handy technique is indispensable for probing the photophysical nature of CQDs and fine-tuning their performance for a variety of applications.

# Chapter 4

## RESULTS AND DISCUSSION

### 4.1 CHARACTERIZATION OF CELLULOSE NANOCRYSTALS (CNC)

#### 4.1.1 Physical Appearance

The physical appearance of the raw material, chemically purified cellulose, and cellulose nanocrystals (CNC) prepared by hydrolysis methods are shown below in Fig.4.1.

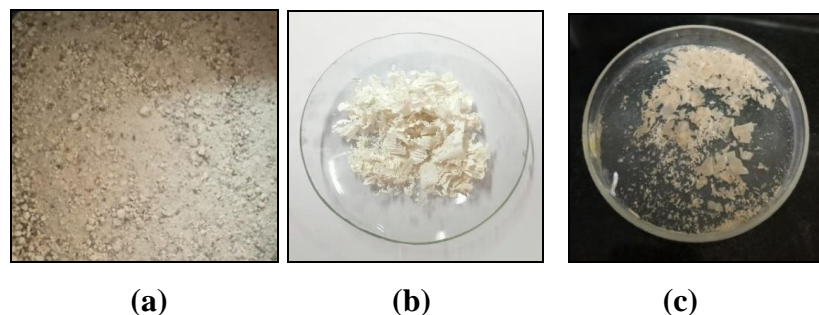


**Fig.4.1: (a) Raw Material , (b) Cellulose , (c) Cellulose Nanocrystals (CNC)**

The alkali pulping and bleaching of the raw material using NaOH and sodium chlorite changed the color and texture of the material. Obtained cellulose is in white color. It indicates the removal of impurities and the presence of maximum cellulose content. Acid hydrolyzed cellulose nanocrystals (CNC) has off white color and crystalline in nature.

#### **4.1.2 X-Ray Diffraction (XRD)**

The X-ray diffraction (XRD) patterns of the raw material, cellulose and cellulose nanocrystals (CNC) are presented in Fig.4.2. A broad peak at approximately  $2\theta = 15^\circ$  was observed in the XRD spectrum of the raw material, indicative of an amorphous arrangement. This broad peak is attributed to the presence of non-cellulosic components, such as lignin and hemicellulose, alongside cellulose. Following treatments such as alkali pulping and bleaching, distinct peaks at  $2\theta$  values of  $15^\circ$ ,  $22^\circ$ , and  $34^\circ$  were observed, corresponding to the characteristic diffraction pattern of cellulose I polymorph. These peaks correspond to the crystallographic planes (110), (002), and (004), respectively. The broad peak observed in the raw material changed into three distinct sharp peaks in cellulose nanocrystals (CNC), indicating the successful removal of non-cellulosic components and confirming the extraction of cellulose. After calculations of the crystallinity index of the raw material, cellulose, cellulose nanocrystals (CNC) using the Segal equation [101]:

$$I_c (\%) = (1 - I_{am} / I_{200}) \times 100\%$$

It was found to be 31.63%, 75.56%, and 78.69% respectively. The increase in crystallinity index of cellulose and cellulose nanocrystals (CNC) is related to increase in ordered region in cellulose and decrease or removal of the amorphous region in raw material [1], [2], [3].

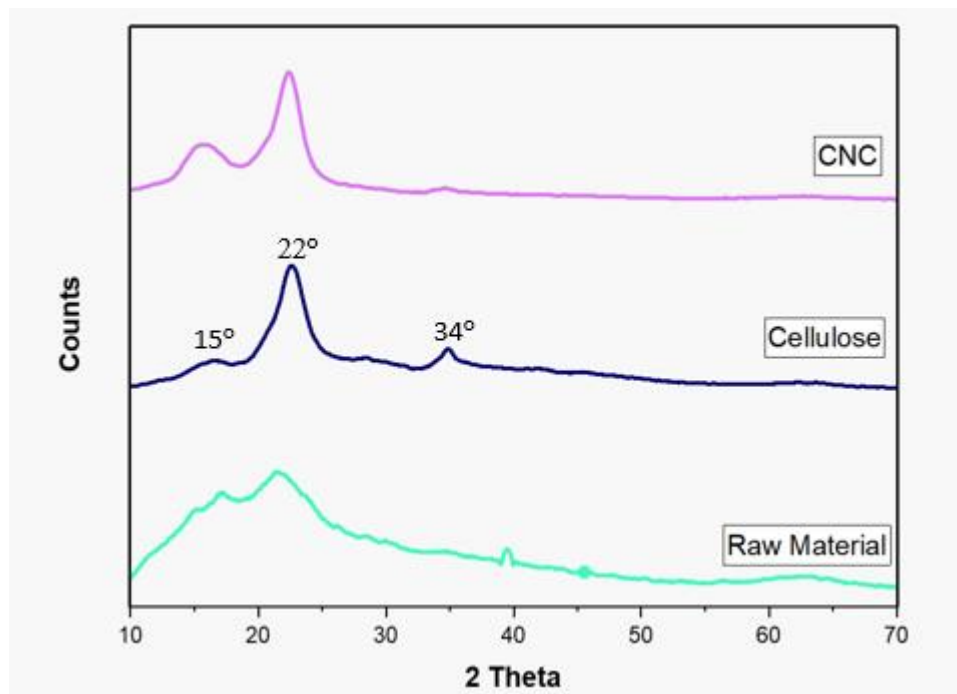


**Fig.4.2: XRD spectra of Raw material, extracted Cellulose and Cellulose Nanocrystals (CNC)**

#### 4.1.3 Fourier Transform Infrared Spectroscopy (FTIR)

FTIR was used to study the changes in functional groups present in raw material, cellulose and cellulose nanocrystals (CNC) after chemical treatments. Fig. 4.3 shows the FTIR spectra obtained at three stages – raw material, cellulose and CNC. The broad peak at  $3417\text{ cm}^{-1}$  corresponds to the O-H stretching bond. The peak observed at  $2923\text{ cm}^{-1}$  in the spectra is due to the C-H stretching vibration in the cellulose molecule. The peak at  $1749\text{ cm}^{-1}$  corresponds to the C-O bond in hemicellulose and lignin in the raw material. This peak disappears in the FTIR of cellulose and cellulose nanocrystals (CNC). The peaks at  $1623\text{ cm}^{-1}$  and  $1248\text{ cm}^{-1}$  indicate the aromatic ring in lignin and C-O stretching in the aryl group of lignin which were removed after the bleaching step that yields cellulose.

The peaks at  $1441\text{ cm}^{-1}$ ,  $1054\text{ cm}^{-1}$  and  $892\text{ cm}^{-1}$  are the characteristic peaks of cellulose which represent O-H bending vibrations, C-O-C pyranose ring stretching vibration and cellulose glycosidic linkage respectively [1], [2], [3]. From this we can conclude the successful removal the non-cellulosic components and extraction of nanocellulose.

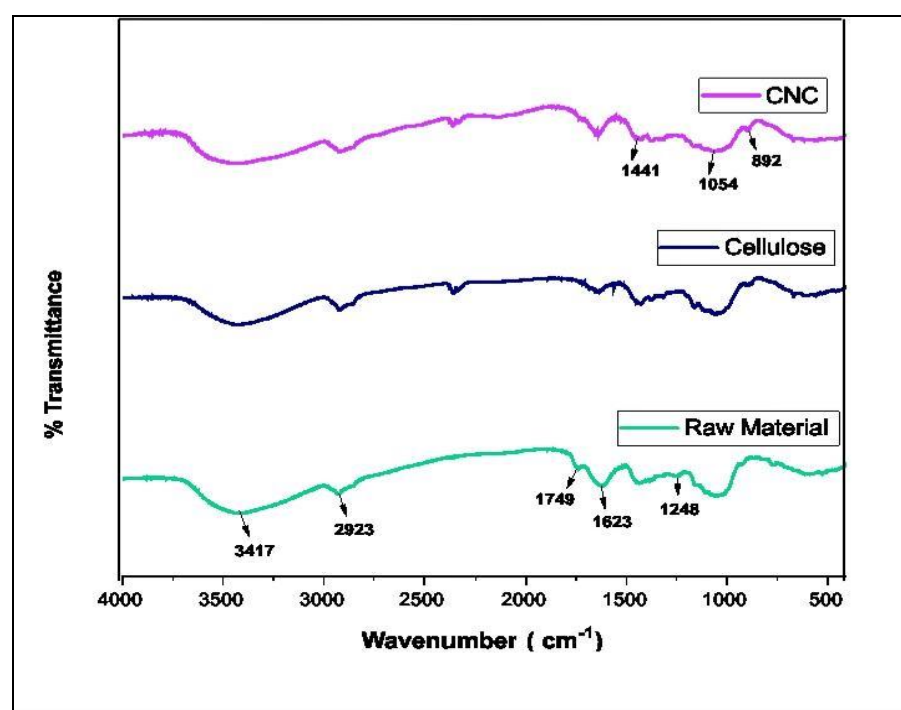


**Fig.4.3: FTIR spectra of Raw material, extracted Cellulose and Cellulose Nanocrystals (CNC)**

#### 4.1.4 Field Emission Scanning Electron Microscopy (FESEM)

FESEM images of raw material as well as the synthesized cellulose and cellulose nanocrystals (CNC) are given in the Fig.4.4. From the FESEM observations we were able to detect the morphological difference between them. It can be seen from the micrographs that raw material has a globular structure since it contains cellulose along with all the non-cellulosic

components. On the other hand cellulose appeared to be in more distinct fiber like structure because of the significant elimination of lignin and hemicellulose in pre-treatments. Cellulose undergo further acid hydrolysis with oxalic acid to form cellulose nanocrystals (CNCs), which have rod-like structures. These rods appears as aggregated clusters because of the strong hydrogen bonding interaction in cellulose nanocrystals (CNC) [1], [2], [3], [4].

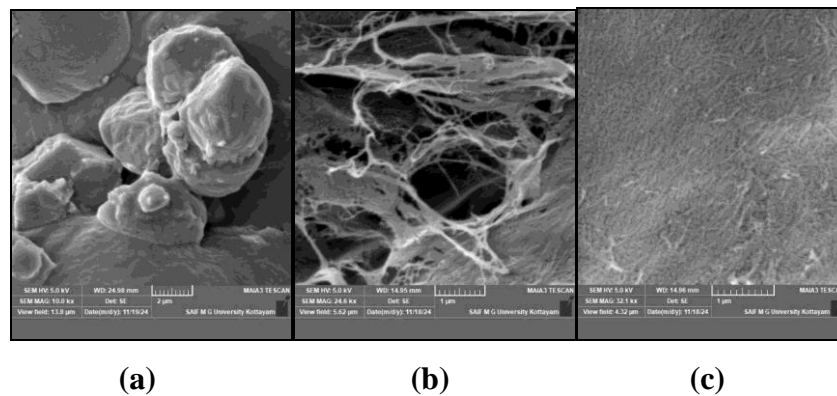


**Fig.4.4: FESEM Images of (a) Raw material, (b) Cellulose, (c) Cellulose nanocrystals (CNC)**

#### 4.1.5 Transmission Electron Microscopy (TEM)

TEM images of cellulose nanocrystals (CNC) derived from jackfruit peels is shown in the Fig 4.5. Cellulose nanocrystals (CNCs) are generally rod-like or needle-shaped, with high aspect ratios characteristic of their nanostructure. In the TEM image, the cellulose nanocrystals (CNCs) appear rod like but mostly as aggregated clusters rather than distinct individual rods. This aggregation likely results from strong intermolecular hydrogen bonding during the drying process, leading to the formation of loosely connected, irregular domains [5].

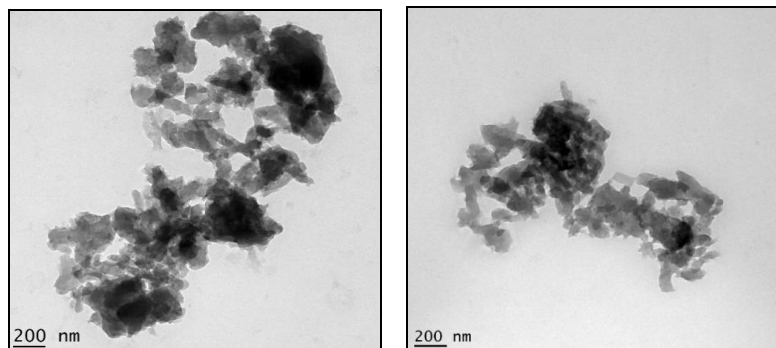


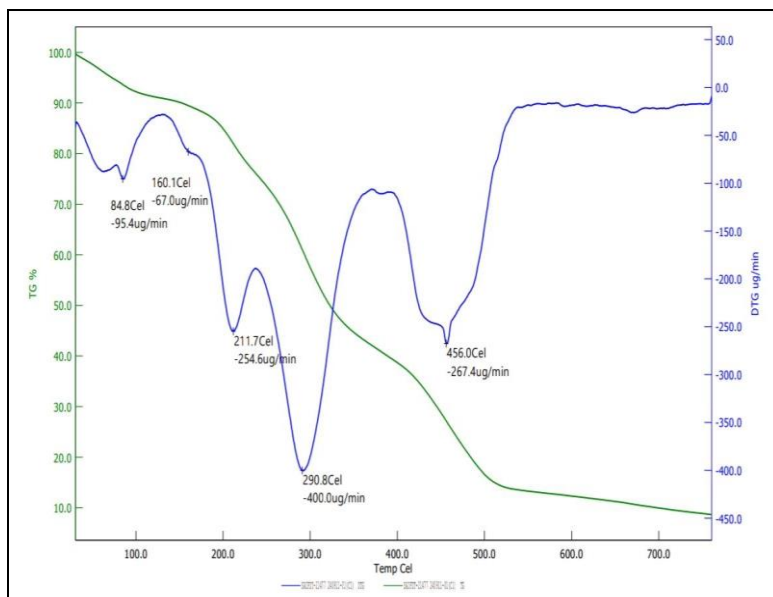
**Fig.4.5: TEM image of Cellulose nanocrystals (CNC)**

#### **4.1.6 Thermogravimetric and Derivative Thermogravimetric Analysis**

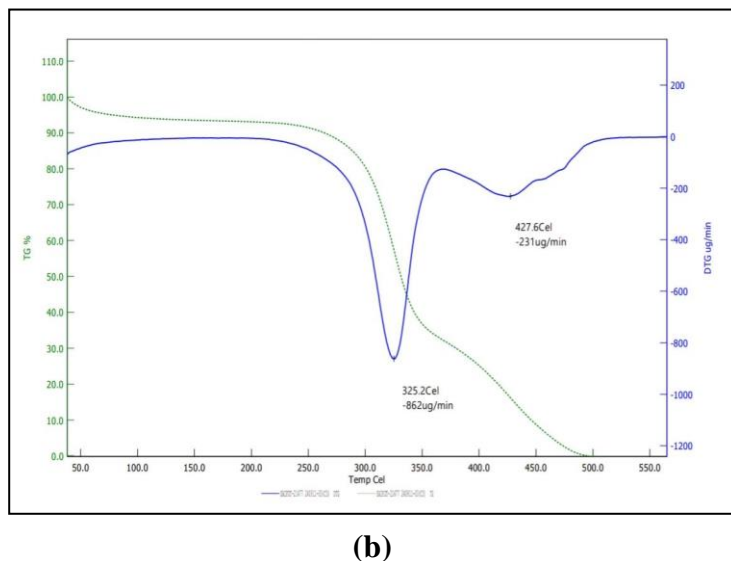
Thermal stability is a crucial factor influencing the behavior of cellulose nanocrystals (CNCs), especially when they are used as reinforcements in various matrices. The thermal characteristics were analyzed by monitoring the mass loss of samples as a function of temperature. A slight weight loss observed around 100°C as shown in Fig.4.6 (a) was attributed to the removal of chemically adsorbed water, which contributes to the cellulose's hydrophilic nature. Additionally, volatile impurities decompose at lower temperatures. The main degradation peak in both raw material as shown in Fig.4.6 (a) and cellulose nanocrystals (CNC) as shown in Fig.4.6 (b) corresponds to the thermal degradation of cellulose. The final degradation peak, observed after 450°C, was linked to the decomposition of lignin and other aromatic compounds. The thermal decomposition of the raw material exhibited several degradation peaks over a wide temperature range, primarily due to the presence of hemicellulose and lignin alongside the cellulose. Cellulose nanocrystals (CNCs), however, do not show this

degradation, indicating that the non-cellulosic components were removed during pretreatment and acid hydrolysis.

The  $T_{max}$  values, obtained from the DTG curve (Fig. 4.6), are 290.8°C for the raw material and 325.2°C for the cellulose nanocrystals (CNCs) indicating increased thermal stability. The thermal instability of the raw material can be primarily attributed to the presence of non-cellulosic components, which are absent in cellulose nanocrystals (CNCs). The increased thermal stability of cellulose nanocrystals (CNCs) after pretreatment and acid hydrolysis is a result of the complete removal of these non-cellulosic regions. Compared to the raw material, cellulose nanocrystals (CNCs) exhibit a  $T_{max}$  increase of 34.4°C. During the conversion of raw material to cellulose nanocrystals (CNC), the disordered cellulose structure is reorganized into a more defined form, contributing to the enhanced thermal stability [106].



(a)



(b)

**Fig.4.6: TGA-DTA of (a) Raw material (b) Cellulose nanocrystals (CNC)**

#### **4.2 DETERMINATION OF ASH AND MOISTURE CONTENT OF CHITIN AND CHITOSAN**

Moisture content is the quantity of water present in a substance. From the obtained result regarding moisture and ash content of chitin or chitosan, moisture content of chitosan (6.8) is less than that of chitin [11]. This difference is due to a change in structure during the conversion of chitin to chitosan by deacetylation process. The solubility of chitosan is attributed to the protonation of amino groups on the polymer chains in acid media, resulting in the destruction of the hydrogen-bonded networks within chitosan molecules by the electrostatic repulsion between positive charges. Due to this process, chitin have lesser affinity towards water than chitin. This results lesser amount of moisture content in chitosan.

Ash content refers to the inorganic residue remaining after either ignition or complete oxidation of organic matter in a substance. Ash content of

chitosan is 1.55, which is lesser than that of chitin which has an ash content of 2.15. This reduction indicates amount of inorganic residue lost during the conversion of chitin to chitosan by the deacetylation process. Ash is an important indicator to evaluate the purity of chitosan and the efficiency of the demineralization process. Chitosan have less ash content due to removal of acetyl groups and minerals during alkaline deacetylation which convert chitin into chitosan.

**Table 4.1: Moisture and Ash Content of Chitin & Chitosan**

Sample	Chitin	Chitosan
Moisture content	11	6.8
Ash content	2.15	1.55

### **4.3 DETERMINATION OF VISCOSITY AND DEGREE OF DEACETYLATION (DDA)**

Viscosity of chitosan is calculated as 445 cps which indicates that polymer matrix used for the synthesis of composite film, chitosan has medium viscosity. The viscosity of chitosan decreases with reducing chitosan molecular weight and is dependent on the polymer's molecular weight and degree of deacetylation. Since a decrease in viscosity is seen during polymer storage as a result of polymer degradation, viscosity can actually be used to determine the stability of the polymer in solution. The

degree of chitosan deacetylation raises viscosity. Polymer matrix in medium viscosity is efficient for the synthesis of composite film.

Degree of Acetylation of chitosan is 75.84% which shows that deacetylation process convert chitin to chitosan by removal of acetyl groups. DDA had a marked effect on the physicochemical properties and affinity of chitosan. Higher DDA value of chitosan showed a greater crystallinity, a higher elastic modulus and tensile strength and a lower swelling.

#### **4.4 CHARACTERIZATION OF PVA/CHITOSAN/CNC NANOCOMPOSITE FILM**

##### **4.4.1 Fourier Transform Infrared Spectroscopy (FTIR)**

The FTIR spectra of both PVA/Chitosan and PVA/Chitosan/1% CNC films are shown in Fig.4.7. In the FTIR spectra of PVA/Chitosan film, a peak corresponding to O-H stretching vibration was observed at  $3310\text{ cm}^{-1}$ . The peak at  $1410.60\text{ cm}^{-1}$  indicates the presence of O-H bending vibration of hydroxyl groups. This implies that a hydrogen bond is formed between the hydroxyl groups of PVA and Chitosan. On analyzing the FTIR spectra of PVA/Chitosan/1% CNC nanocomposite film, it was observed that a peak corresponding to O-H stretching vibration was found at  $3300\text{ cm}^{-1}$  due to the incorporation of CNC into the PVA/Chitosan blend. These results reveal strong electrostatic interactions and hydrogen bonding between CNC's functional groups and available functional groups of PVA/Chitosan polymer blend [6]. The peaks at  $1055\text{ cm}^{-1}$  and  $851.76\text{ cm}^{-1}$  indicates the presence of C-O-C pyranose ring stretching vibration and cellulosic  $\beta$ -glycosidic linkages respectively which in turn implies that the CNCs were incorporated into the PVA/Chitosan blend [3].

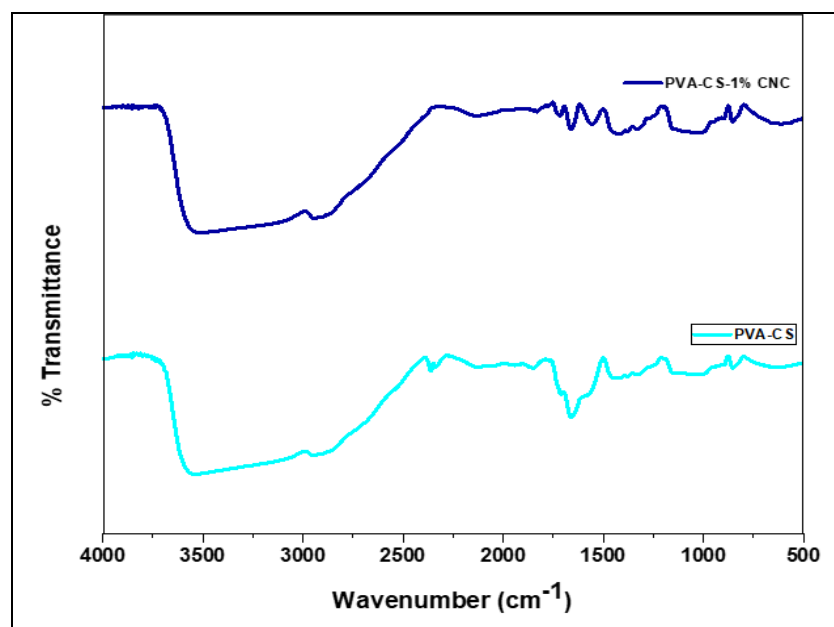


**Fig. 4.7: FTIR spectra of PVA/Chitosan and PVA/Chitosan/CNC nanocomposite films**

#### 4.4.2 Field Emission Scanning Electron Microscopy (FESEM)

Morphological analysis of the prepared PVA/Chitosan and PVA/Chitosan/1% CNC composite films were performed using field emission scanning electron microscopy as shown in Fig.4.8. FESEM provides high resolution imaging that allows for the analysis of material morphology and microstructure. This includes examining voids, assessing homogeneity, identifying the presence of aggregates, and evaluating nanoparticle distribution and orientation. It revealed that the PVA/Chitosan film surface was regular and uniform without any flaw, confirming the compatibility of PVA and Chitosan polymeric matrix. The even surface of the blend film suggests uniform dispersion in the matrix, which may be attributed to hydrogen bond formation between the hydroxyl and amino groups of CS and hydroxyl groups of PVA. From the

images random orientation and good dispersion of CNC in the matrices were observed. These results indicate excellent compatibility among the three components of each nanocomposite. Also the addition of CNC altered the film's microstructure, and it resulted in a uniformly dispersed matrix.

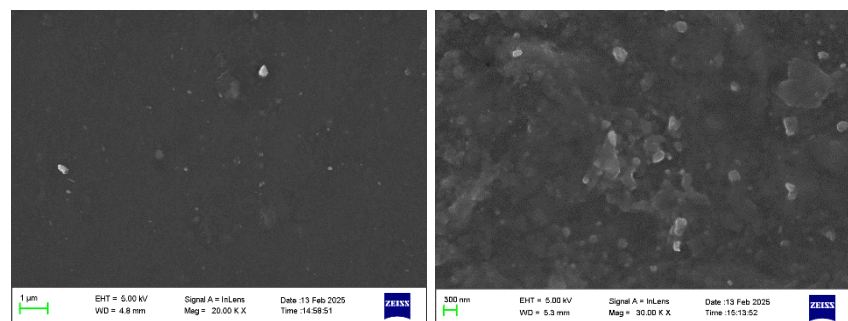


**Fig.4.8: FESEM Images of (a) PVA/CS and (b) PVA/CS/1% CNC nanocomposite films**

#### 4.4.3 Mechanical Properties (Tensile strength)

The addition of cellulose nanocrystals (CNC) into the PVA/CS matrix is a significant factor in determining the mechanical strength of the composite films. The tensile strength of the pure PVA/CS film was 13.878 MPa, which means it performed at a basic level. When cellulose nanocrystals (CNC) was added at 1% concentration, the tensile strength increased to 18.364 MPa, which indicates that the incorporation of cellulose nanocrystals (CNC) is a supplementary task to the far stronger film structure, likely through a better dispersions and reinforcements from the cellulose nanocrystals (CNC) particles. Despite this, with the cellulose nanocrystals (CNC) concentration risen to 3% and 5%, the tensile strength showed a downward trend, providing less than average values of 12.522 MPa and 9.046 MPa, respectively. This fall of mechanical strength, when the cellulose nanocrystals (CNC) loading was higher, can be due to the

poor dispersion or agglomeration of cellulose nanocrystals (CNC), causing structural inconsistencies that weaken the film. Also, at higher cellulose nanocrystals (CNC) concentrations, the authority of the matrix to properly move stress through the cellulose nanocrystals (CNCs) could be less, and thus, the tensile strength could be lost [7], [8]. The results of this study underscore the need to optimize the 1% cellulose nanocrystals (CNC) content to have better reinforcement properties for packaging application.

#### **4.5 APPLICATIONS OF PVA/CHITOSAN/CNC NANOCOMPOSITE FILMS**

##### **4.5.1 Impact of PVA/ Chitosan/CNC film on Curry Leaf Freshness and Shelf Life**

The effect of PVA/Chitosan/CNC nanocomposite film on the preservation of curry leaves was observed over a period of 57 hours and compared to unwrapped leaves kept under identical conditions. At 0 hours, both wrapped and unwrapped leaves displayed similar freshness and vibrancy. However, within the first 3 hours, the unwrapped leaves showed initial signs of wilting, while the wrapped leaves maintained their moisture and color. This trend continued, with the unwrapped leaves displaying significant wilting and reduced vibrancy by the 9-hour mark, whereas the wrapped leaves retained a relatively fresh appearance. By 22 hours, the unwrapped leaves exhibited pronounced wilting and darkening, while the wrapped leaves showed minimal degradation. At 24 and 57 hours, the wrapped leaves still retained their structure, color, and moisture noticeably better than the unwrapped leaves, which had become dry, brittle, and visibly darker. Comparing the wrapped leaves 1% film shows better preservation properties than other films as shown in Fig.4.9. This comparison demonstrates that the PVA/Chitosan/1% CNC nanocomposite

film acts as an effective preservation barrier, slowing moisture loss and oxidation, and thus prolonging the freshness of the leaves.

To enhance the packaging properties and shelf life, the films were further incorporated with nanocurcumin and lemon grass essential oil. For this preparation of nanocomposite film was altered by introducing 0.2g nanocurcumin and 1 mL lemon grass oil in the blending step.

When observed in similar conditions and time intervals as in PVA/Chitosan and PVA/Chitosan/CNC nanocomposite films, curry leaves wrapped in altered films shows better properties and minimal degradation. Film made with lemon grass oil has better preservation properties than nanocurcumin loaded film. Curry leaves wrapped in nanocurcumin based film maintained freshness for 120 hours while lemon grass oil incorporated film remained as fresh till 144 hours as shown in Fig.4.10. This finding highlights the potential of PVA/Chitosan/CNC films as sustainable and biodegradable alternatives for extending the shelf life of perishable plant materials [9].

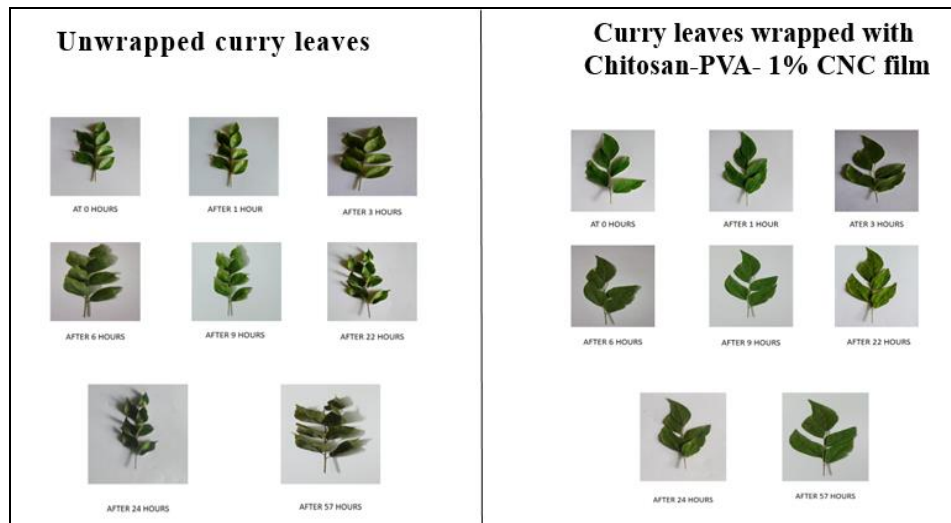


**Fig.4.9: Visual comparison of curry leaves over 57 hours unwrapped leaves and leaves wrapped in PVA/Chitosan/ 1% CNC nanocomposite film.**

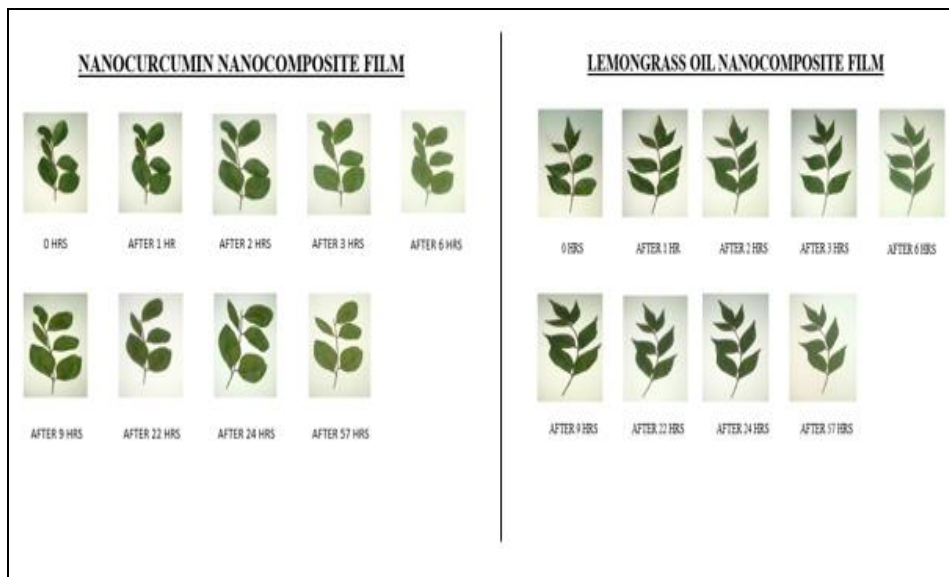


**Fig.4.10: Visual comparison of curry leaves over 57 hours wrapped in nanocurcumin nanocomposite film and leaves wrapped in lemon grass oil nanocomposite film**

#### **4.5.2 Application of PVA/ Chitosan/CNC Nanocomposite Film in Oil Spill Remediation**

A successful cleanup of oil spills must always be done in order to lessen environmental, economic, and social impacts caused by a spill. It is also worth noting that if cleaning is done properly and timely, it can minimize the effects on marine life, maintain natural habitats, and preserve the quality of water. In addition, remediation is able to reduce the overall economic effects by protecting fisheries, tourism, and coastal properties and minimizing the associated costs of restoration. Most importantly, oil spill remediation would alleviate human suffering, prevent people from losing a source of income, ensure that legal demands are followed thus making the environment safer for future generations.

The PVA/Chitosan/CNC nanocomposite film demonstrated remarkable oil adsorption properties when placed in a petrol-water mixture, highlighting its potential for environmental applications such as oil spill remediation.

To study the oil adsorption properties of the nanocomposite film, hydrocarbon analysis was performed. For this water sampling was conducted on 3 water bodies near refineries and oil spill prone areas in Kochi Estuary. The concentration of dissolved oxygen was determined in order to evaluate the water quality on each station. The dissolved oxygen (DO) levels were determined using the Winkler method. For this water sample was filled fully in a BOD bottle without any gap left for air and 2 mL of manganese sulfate and 2 mL of alkali-iodide-azide reagent were added. After mixing, a precipitate formed and was dissolved by adding 2 mL of concentrated sulfuric acid. The treated sample was then titrated with sodium thiosulfate until a pale straw color appeared. 1 mL of starch

solution was added, turning the solution blue. Titration continued until the blue color disappeared. The DO concentration was then calculated.

**Table 4.2 DO value of water from the three sampling stations**

Sampling Station	Dissolved Oxygen (DO) (ml/l)
Fort Kochi Boat Jetty	3.83
North Tanker Berth of Cochin Port Trust	7.67
Vypin Boat Jetty	3.83

The DO value between 6-8 indicates that the water is usable and the value below 6 shows the amount of pollution in water bodies. Thus the two of the observed station has very low dissolved oxygen and hence it's polluted from hydrocarbons and many other pollutants.

PVA/Chitosan/1% CNC nanocomposite film treatment was done on these water samples to remove hydrocarbons and in turn to observe and study its adsorption properties. Two sets of water sample each of 500ml was taken from each stations. Hexane was used as the solvent to extract petroleum hydrocarbons from water by Total hydrocarbon extraction. For this 500ml of water sample from each station was taken in 3 clean, dry separating funnel respectively. To this 25 ml of hexane was added and shaken vigorously for 5 minutes.

It was then allowed to stand undisturbed to separate into aqueous layer and organic layer. From this aqueous layer was drained and the hexane layer containing hydrocarbons was collected. This process was repeated three times with fresh hexane to maximum recovery. The

PVA/Chitosan/1% CNC nanocomposite film was deployed over the hexane layer to examine its oil adsorption properties. The collected hexane layer was analyzed using spectrofluorometer to quantify the hydrocarbons present. Concentration of Hydrocarbon in hexane layer of untreated water sample was also analyzed. Table 4.3 below shows the hydrocarbon concentration studied using spectrophotometric analysis.

**Table 4.3 Hydrocarbon concentration of the collected water samples**

<b>Sampling Station</b>	<b>Concentration of Hydrocarbon Before Film Treatment</b>	<b>Concentration of Hydrocarbon After Film Treatment</b>	<b>% of Adsorption</b>
Fort Kochi Boat Jetty	164.2	79.3	51.7%
North Tanker Berth of Cochin Port Trust	147	85.9	41.56%
Vypin Boat Jetty	91.9	47.1	48.74%

The results clearly marks approximately 50% oil absorption efficiency for PVA/Chitosan/1% CNC nanocomposite film making it a better candidate as an eco-friendly solution for oil spill cleanup and wastewater treatment.

### 4.3 CELLULOSE PAPER

Cellulose paper as shown in Fig.4.11 was synthesized from the cellulose residue derived from jackfruit peels is a green and sustainable alternative to traditional paper. This new cellulose paper thus minimizes wood based paper and has potential applications in green packaging, biodegradable paper products, and ecofriendly printing materials.

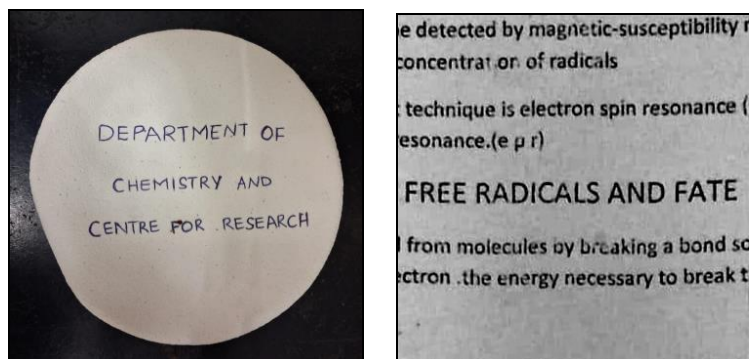


**Fig.4.11: Printable Cellulose Paper**

### 4.6 CHARACTERIZATION TECHNIQUES OF CARBON QUANTUM DOTS (CQDs)

#### 4.6.1 UV-VIS spectroscopy

The UV-Vis spectrum shown here in Fig 4.12 presents the absorbance properties of carbon quantum dots (CQDs).

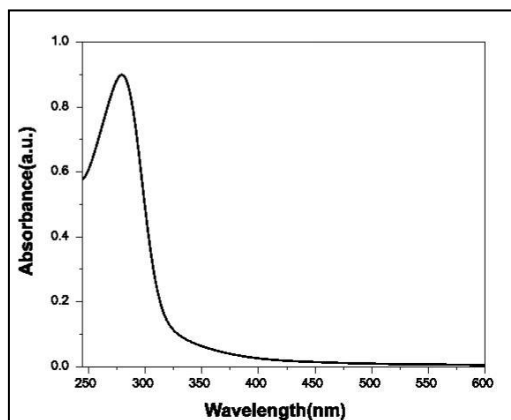


**Fig 4.12: UV-VIS Spectra of Carbon Quantum Dots (CQDs)**

The spectrum has a very intense absorption band at 279.7 nm, typical of the  $\pi-\pi^*$  transition of aromatic C=C bonds in conjugated systems. The appearance of this band suggests the presence of  $sp^2$  hybridized carbon structures, possibly from graphitic domains in the carbon quantum dots (CQDs). It is possible to observe a flat peak around 340 nm, which has been assigned to the  $n-\pi^*$  transitions of C=O chromophore of different functional groups widely seen in the structure of the CQDs.

#### 4.6.2 Photo Luminescence Spectroscopic Technique

The photoluminescence (PL) spectra of carbon quantum dots (CQDs), as indicated in the given (Fig.4.13), are characterized by strong excitation-dependent emission behavior. The spectra show several emission peaks with different intensities based on the excitation wavelength, ranging from 260 nm to 400 nm. The maximum intensity is found at lower excitation wavelengths, indicating a strong fluorescence response in the UV range. The wide emission bands reflect the occurrence of several emissive states, which may be due to surface functional groups, quantum confinement effects, or various sizes of carbon nano domains. The redshift of emission maxima with rising excitation

wavelength is typical of carbon quantum dots and reflects a distribution of energy states in the material.

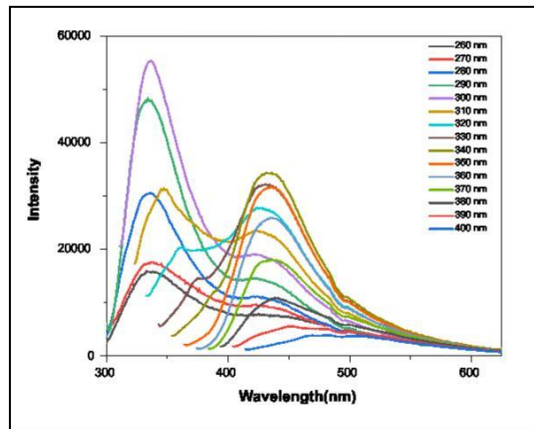


**Fig 4.13: PL spectra of Carbon Quantum Dots (CQDs)**

## 4.7 APPLICATIONS OF CARBON QUANTUM DOTS

### 4.7.1 ANTIOXIDANT ANALYSIS

$$\text{Percentage of DPPH scavenging activity} = \frac{\text{Abs of control} - \text{Abs of sample}}{\text{Abs of control}} \times 100$$

#### SAMPLE 1

$$\text{Absorbance of control (DPPH)} = \mathbf{2.4017}$$

$$\text{Absorbance of sample 1a} = 0.2034$$

$$\text{Absorbance of sample 1b} = 0.1998$$

$$\begin{aligned} \text{Average absorbance} &= (0.2034+0.1998)/2 = 0.4032/2 \\ &= \mathbf{0.2016} \end{aligned}$$

$$\begin{aligned} \text{Percentage of DPPH scavenging activity} &= \frac{2.4017 - 0.2016}{2.4017} \times 100 \\ &= \frac{2.2001}{2.4017} \times 100 \end{aligned}$$

$$= 0.9160 \times 100$$

**Percentage of DPPH scavenging activity = 91.6 %**

#### **4.7.2 FLUORESCENT INK**

The use of CQDs as luminous ink because of their excellent qualities, such as their dispersion, water solubility, and strong fluorescence, carbon quantum dots have found application in a wide range of industries. The usage of fluorescent ink with carbon quantum dots has been covered in a number of articles. The potential use of CQDs as invisible fluorescent ink was examined in this study. Without any changes, the CQD aqueous solution was transferred into a pen. Subsequently, various texts, designs, and patterns were inscribed on a filter paper. Both daylight and ultraviolet light caused the digital images to emit. With direct light, the letters were colorless, but with UV irradiation, the bright blue fluorescence letters were apparent. The resulting fluorescent ink was also easily removable, nontoxic, transparent, and persistent. The produced carbon quantum dots may therefore find application in the fields of anticounterfeiting and luminous pens.

# Chapter 5

## CONCLUSION

The reuse, recycling, and recovery of various biomass waste for high-value-added products have received great attention in reducing the environmental impact and pollution. This project work explored the transformation of jackfruit peels, a widely available but underutilized agro-waste, into two value added products: cellulose nanocrystals (CNC) and carbon quantum dots (CQDs). Cellulose nanocrystals (CNCs) are nanomaterials made from cellulose, a natural polymer found in plant cell walls. They have high surface area and mechanical strength. They are biodegradable, renewable and nontoxic. Whereas carbon quantum dots, a novel member of carbon family, are recently emerging as a potential substitute for traditional fluorescent materials. CQDs derived from waste materials are drawing much attention due to their distinct features such as cost-effectiveness, nontoxic nature, tunable luminescence, good water solubility and high biocompatibility.

By applying the “Waste to Wealth” principle, the study focus on issues of waste management and environmental sustainability, and present its potential to transform organic waste into valuable, high-performance materials.

The jackfruit peels were subjected to a three-stage process: alkali pulping, bleaching, and acid hydrolysis. These steps effectively removed non-cellulosic components such as lignin and hemicellulose, yielding highly

pure cellulose and subsequently nanocellulose. Analytical techniques, including X-ray Diffraction (XRD), Fourier-Transform Infrared spectroscopy (FTIR), Field Emission Scanning Electron Microscopy (FESEM), and Transmission Electron Microscopy (TEM), confirmed the successful synthesis of cellulose nanocrystals (CNC). The analysis shows that the extracted cellulose nanocrystals (CNC) exhibited high crystallinity, enhanced thermal stability, and improved mechanical properties, validating the efficiency of the process.

The extracted cellulose nanocrystals (CNC), with its nanoscale structure, presented exceptional properties such as high surface area, biocompatibility, and biodegradability. These properties were leveraged to create PVA/Chitosan/CNC composite films with significant potential for industrial applications. The films demonstrated enhanced mechanical strength and barrier properties, making them highly suitable for sustainable food packaging. When applied to study the degradation of curry leaves, the films successfully extended their shelf life by preserving freshness and minimizing moisture loss. Further modifications, such as incorporating nanocurcumin and lemongrass essential oil, significantly enhanced the preservation capabilities of the films. These variations extended the freshness of curry leaves for up to 144 hours, showcasing the potential of the nanocomposite in prolonging the shelf life of plant parts.

The project further emphasized the eco-friendly nature of the processes used. Since the acid used for hydrolysis is mild and non-toxic oxalic acid, the research minimized the environmental impact from the conventional methods using harsh chemicals. This emphasis on green chemistry ensures not only environmental safety but also achieves the goals of sustainable development.

The applications of cellulose nanocrystals (CNCs) go beyond food packaging and environmental remediation. Its high surface area and chemical modifiability further expand its utility in areas such as water purification, catalysis, dye degradation and the development of advanced nanocomposite.

This research shows that agricultural waste, such as jackfruit peels, can be transformed into highly valuable cellulose nanocrystals (CNCs), thereby giving a more sustainable means of waste management while promoting material science. The process of transforming waste into useful products fits into global goals toward sustainability and environmental conservation. It has also been seen that cellulose nanocrystals (CNCs) have vast potential as a green material for applications such as packaging, water purification, and healthcare. Future research may focus on improving the production process to achieve industrial scalability, investigating other sources of agro-waste, and discovering new applications, including flexible electronics and renewable energy. Accepting cellulose nanocrystals (CNCs) as a sustainable alternative to non-biodegradable materials may revolutionize industries and support a greener, more sustainable future.

Using a multi-step procedure that included deproteinization with 1M NaOH, demineralization with HCl, and decolorization with a methanol-water-chloroform mixture, chitin was recovered from shrimp shell waste. After that, chitosan was separated from chitin by deacetylating it with 50% NaOH. Using common laboratory techniques, such as oven drying and muffle furnace heating, the resultant chitin and chitosan were characterized by measuring their ash and moisture content. Because of the structural alterations brought about by the deacetylation process, chitosan has a lower moisture content (6.8%) than chitin (11%). Additionally, chitosan's ash

percentage (1.55%) was lower than chitin's (2.15%), suggesting that inorganic residues were eliminated throughout the conversion process. Chitosan was discovered to have a medium viscosity of 445 cps, which is appropriate for the synthesis of composite films. Chitosan's degree of deacetylation (DDA) was 75.84%, indicating that chitin was effectively converted to chitosan. The findings imply that chitosan's physicochemical characteristics are influenced by the deacetylation process, which renders it appropriate for a range of uses.

In given study on PVA/Chitosan/CNC nanocomposite film, remarkable oil absorption properties was shown in petrol-water mixtures. Near refineries and areas prone to oil spills namely cleaning and isolating spills of oil can mitigate environmental, economic, and social impacts and protect marine life, thus maintaining water quality and reducing economic effects from impeding fishing, tourism, and coastal properties. A hydrocarbon analysis on water bodies was done, extracting petroleum hydrocarbons via hexane. The nanocomposite film demonstrated an impressive oil absorption efficiency of about 51.7%, rendering a promising eco-friendly solution for oil spill remediation. This study brings out the usefulness of nanocomposite films in environmental applications. Their application in oil spill cleanup demonstrated exceptional oil absorption capabilities, highlighting their potential in mitigating environmental pollution in water bodies affected by hydrocarbon contamination.

Since hydrothermal synthesis is a method that varies mainly according to the reaction conditions and the solvent used, it is one of the most popular methods for preparing carbon quantum dots (CQDs) from cellulose. Hydrothermal synthesis refers to a process whereby at high temperatures and under high pressures (120–280°C), the cellulose or its derivatives

carbonize, nucleate, and produce carbon quantum dots in a closed system with water as the medium. This method is popular for cellulose-based CQDs because it is cheap, easy to perform, and has no harmful effects on the environment.

The UV- Visible spectra show intense absorption bands at 279.7 nm related to  $sp^2$  hybridized carbon structures and an  $n-\pi^*$  transition of the carbonyl chromophore in the structure of CQDs with a flat peak at 340 nm. This indicates the formation of carbon quantum dots (CQDs).

The photoluminescence spectra of carbon quantum dots show the excitation-dependent emission characteristics very strongly that vary in intensity with the excitation wavelength. The very lowest wavelengths give the maximum response, indicating a good UV fluorescence response. The redshift of emission maxima represents the energy states distribution in the material.

The percentage of DPPH scavenging activity was calculated and observed that the synthesized carbon quantum dots showed 91.6% efficiency. This indicates that they have significant antioxidant activity.

The ability of CQDs to work as non-visible fluorescent ink was evaluated. An ink that was fluorescent was done by preparing an aqueous CQD solution and filled in an ink pen, writing various characters and designs on filter paper. It turned out the fluorescent ink, a non-toxic, transparent, and permanent ink, is a possible means of anticounterfeiting and can be used for luminous pens.

Cellulose which is an important intermediate during the synthesis of cellulose nanocrystals from jackfruit peels was casted into a petridish to

obtain cellulose paper which is an alternative to the conventional paper. So the intermediate was also transformed into a value added product.

To conclude, this project work include innovative strategy, which integrates waste management with the synthesis of two high value added multifunctional materials – cellulose nanocrystals (CNC) and carbon quantum dots (CQDs), which offers a pioneering approach to sustainability, enabling the creation of economy that minimizes waste and maximizes value.

## References

---

- [1] R. Benton, “Reduce, Reuse, Recycle ... and Refuse,” *J. Macromarketing*, vol. 35, no. 1, pp. 111–122, 2014, doi: 10.1177/0276146714534692.
- [2] A. Antony and R. thottiam Vasudevan, “EXTRACTION AND FUNCTIONAL PROPERTIES OF CELLULOSE FROM JACKFRUIT (ARTOCARPUS INTEGER) WASTE,” *Int. J. Pharm. Sci. Res.*, vol. 9, pp. 4309–4317, 2018, doi: 10.13040/IJPSR.0975-8232.9(10).4309-17.
- [3] M. H. Rubiyah *et al.*, “Isolation and characterization of cellulose nanofibrils from agro-biomass of Jackfruit (Artocarpus heterophyllus) rind, using a soft and benign acid hydrolysis,” *Carbohydr. Polym. Technol. Appl.*, vol. 6, p. 100374, 2023, doi: <https://doi.org/10.1016/j.carpta.2023.100374>.
- [4] R. J. Najy, “Reverse Processing Series System Integration with Cleaner Production Processes in Iraqi Industrial Companies,” 2021.
- [5] R. Brahma and S. Ray, “Optimization of extraction conditions for cellulose from jackfruit peel using RSM, its characterization and comparative studies to commercial cellulose,” *Meas. Food*, vol. 13, p. 100130, 2024, doi: <https://doi.org/10.1016/j.meafoo.2023.100130>.
- [6] D. Trache *et al.*, “Nanocellulose: From Fundamentals to Advanced Applications,” *Front. Chem.*, vol. 8, 2020, [Online]. Available: <https://www.frontiersin.org/journals/chemistry/articles/10.3389/fchem.2020.00392>

- [7] H. Richards, P. Baker, and E. Iwuoha, “Metal Nanoparticle Modified Polysulfone Membranes for Use in Wastewater Treatment: A Critical Review,” *J. Surf. Eng. Mater. Adv. Technol.*, vol. 2, p. 183, 2012, doi: 10.4236/jsemat.2012.223029.
- [8] H. Flint, K. Scott, S. Duncan, P. Louis, and E. Forano, “Microbial degradation of complex carbohydrates in the gut,” *Gut Microbes*, vol. 3, pp. 289–306, 2012, doi: 10.4161/gmic.19897.
- [9] D. Lavanya, P. Kulkarni, M. Dixit, P. K. Raavi, and L. N. V Krishna, “Sources of cellulose and their applications- A review,” *Int. J. Drug Formul. Res.*, vol. 2, pp. 19–38, 2011.
- [10] D. Trache, M. H. Hussin, M. K. M. Haafiz, and V. K. Thakur, “Recent progress in cellulose nanocrystals: sources and production,” *Nanoscale*, vol. 9, no. 5, pp. 1763–1786, 2017, doi: 10.1039/C6NR09494E.
- [11] X. Tang, G. Liu, H. Zhang, X. Gao, M. Li, and S. Zhang, “Facile preparation of all-cellulose composites from softwood, hardwood, and agricultural straw cellulose by a simple route of partial dissolution,” *Carbohydr. Polym.*, vol. 256, p. 117591, 2021, doi: <https://doi.org/10.1016/j.carbpol.2020.117591>.
- [12] E. Kalita, B. K. Nath, F. Agan, V. More, and P. Deb, “Isolation and characterization of crystalline, autofluorescent, cellulose nanocrystals from saw dust wastes,” *Ind. Crops Prod.*, vol. 65, pp. 550–555, 2015, doi: <https://doi.org/10.1016/j.indcrop.2014.10.004>.
- [13] H. C. Chan, C. H. Chia, S. Zakaria, I. Ahmad, and A. Dufresne, “Production and characterisation of cellulose and nano-crystalline cellulose from kenaf core wood,” *BioResources*, vol. 8, no. 1, pp. 785–794, 2012.
- [14] C. A. de Carvalho Mendes, N. M. S. Ferreira, C. R. G. Furtado, and

A. M. F. de Sousa, “Isolation and characterization of nanocrystalline cellulose from corn husk,” *Mater. Lett.*, vol. 148, pp. 26–29, 2015.

[15] H. D. Nguyen, T. T. T. Mai, N. B. Nguyen, T. D. Dang, M. L. P. Le, and T. T. Dang, “A novel method for preparing microfibrillated cellulose from bamboo fibers,” *Adv. Nat. Sci. Nanosci. Nanotechnol.*, vol. 4, no. 1, p. 15016, 2013.

[16] R. PK, M. MS, A. Sunil, A. KS, J. Joseph, and J. TU, “Synthesis and characterization of nanocellulose from watermelon rinds and water hyacinth,” *Polym. from Renew. Resour.*, vol. 14, no. 3, pp. 157–172, 2023.

[17] E. S. Abdel-Halim, “Chemical modification of cellulose extracted from sugarcane bagasse: Preparation of hydroxyethyl cellulose,” *Arab. J. Chem.*, vol. 7, no. 3, pp. 362–371, 2014.

[18] A. Kumar, Y. Negi, V. Choudhary, and N. Bhardwaj, “Characterization of Cellulose Nanocrystals Produced by Acid-Hydrolysis from Sugarcane Bagasse as Agro-Waste,” *J. Mater. Phys. Chem.*, vol. 2, pp. 1–8, 2014, doi: 10.1007/978-3-642-27758-0\_1162-2.

[19] E. Suter, W. Omwoyo, O. Nathan, and M. J. Moloto, “Chemically purified cellulose and its nanocrystals from sugarcane baggase: isolation and characterization,” *Heliyon*, vol. 5, p. e02635, 2019, doi: 10.1016/j.heliyon.2019.e02635.

[20] Y. Van Daele, J. Revol, F. Gaill, and G. Goffinet, “Characterization and supramolecular architecture of the cellulose-protein fibrils in the tunic of the sea peach (*Halocynthia papillosa*, Ascidiacea, Urochordata),” *Biol. Cell*, vol. 76, no. 1, pp. 87–96, 1992.

[21] G. Song *et al.*, “Structure and composition of the tunic in the sea

pineapple *Halocynthia roretzi*: A complex cellulosic composite biomaterial,” *Acta Biomater.*, vol. 111, pp. 290–301, 2020.

[22] Y. Zhao and J. Li, “Excellent chemical and material cellulose from tunicates: diversity in cellulose production yield and chemical and morphological structures from different tunicate species,” *Cellulose*, vol. 21, no. 5, pp. 3427–3441, 2014, doi: 10.1007/s10570-014-0348-6.

[23] S. Steven, Y. Mardiyati, S. Shoimah, R. R. Rizkiansyah, S. Santosa, and R. Suratman, “Preparation and Characterization of Nanocrystalline Cellulose from *Cladophora* sp. Algae,” *Int. J. Adv. Sci. Eng. Inf. Technol.*, vol. 11, p. 1035, 2021, doi: 10.18517/ijaseit.11.3.10278.

[24] N. Schultz-Jensen *et al.*, “Pretreatment of the macroalgae *Chaetomorpha linum* for the production of bioethanol—comparison of five pretreatment technologies,” *Bioresour. Technol.*, vol. 140, pp. 36–42, 2013.

[25] P. Nova *et al.*, “Chemical Composition and Antioxidant Potential of Five Algae Cultivated in Fully Controlled Closed Systems,” *Molecules*, vol. 28, p. 4588, 2023, doi: 10.3390/molecules28124588.

[26] T. Itoh and R. M. Brown, “Development of cellulose synthesizing complexes in *Boergesenia* and *Valonia*,” *Protoplasma*, vol. 144, pp. 160–169, 1988.

[27] T. Itoh, “Cellulose synthesizing complexes in some giant marine algae,” *J. Cell Sci.*, vol. 95, no. 2, pp. 309–319, 1990.

[28] H. Kargarzadeh *et al.*, “Recent developments in nanocellulose-based biodegradable polymers, thermoplastic polymers, and porous nanocomposites,” *Prog. Polym. Sci.*, vol. 87, pp. 197–227, 2018,

doi: <https://doi.org/10.1016/j.progpolymsci.2018.07.008>.

[29] A. Shafiq *et al.*, “Lignin derived polyurethanes: Current advances and future prospects in synthesis and applications,” *Eur. Polym. J.*, vol. 209, p. 112899, 2024, doi: <https://doi.org/10.1016/j.eurpolymj.2024.112899>.

[30] A. D. French, S. Pérez, V. Bulone, T. Rosenau, and D. Gray, “Cellulose,” in *Encyclopedia of Polymer Science and Technology*, 2018, pp. 1–69, doi: <https://doi.org/10.1002/0471440264.pst042.pub2>.

[31] P. Kaur *et al.*, “Nanocellulose: Resources, Physio-Chemical Properties, Current Uses and Future Applications,” *Front. Nanotechnol.*, vol. 3, 2021, doi: 10.3389/fnano.2021.747329.

[32] C. Salas, T. Nypelö, C. Rodriguez-Abreu, C. Carrillo, and O. J. Rojas, “Nanocellulose properties and applications in colloids and interfaces,” *Curr. Opin. Colloid Interface Sci.*, vol. 19, no. 5, pp. 383–396, 2014, doi: <https://doi.org/10.1016/j.cocis.2014.10.003>.

[33] R. Trivedi and P. Prajapati, “CHAPTER 3 - Nanocellulose in packaging industry,” in *Micro and Nano Technologies*, R. Oraon, D. Rawtani, P. Singh, and D. C. M. B. T.-N. M. Hussain, Eds., Elsevier, 2022, pp. 43–66. doi: <https://doi.org/10.1016/B978-0-12-823963-6.00012-0>.

[34] R. K. Mishra, A. Sabu, and S. K. Tiwari, “Materials chemistry and the futurist eco-friendly applications of nanocellulose: Status and prospect,” *J. Saudi Chem. Soc.*, vol. 22, no. 8, pp. 949–978, 2018.

[35] R. S. Dhesingh, “Cellulose Nanocrystals for Health Care Applications,” 2018, pp. 415–459. doi: 10.1016/B978-0-08-101971-9.00015-6.

[36] A. S. Norfarhana *et al.*, “Exploring of Cellulose Nanocrystals from

Lignocellulosic Sources as a Powerful Adsorbent for Wastewater Remediation,” *J. Polym. Environ.*, pp. 1–31, 2024.

[37] W. Chen, H. Yu, Y. Liu, P. Chen, M. Zhang, and Y. Hai, “Individualization of cellulose nanofibers from wood using high-intensity ultrasonication combined with chemical pretreatments,” *Carbohydr. Polym.*, vol. 83, no. 4, pp. 1804–1811, 2011, doi: <https://doi.org/10.1016/j.carbpol.2010.10.040>.

[38] A. Thirumalai, A. Girigoswami, and K. Girigoswami, “Bacterial nanocellulose-Robust preparation and application—A literature review,” *Appl. Chem. Eng.*, vol. 6, 2023, doi: 10.24294/ace.v6i3.2170.

[39] J. Xue, T. Wu, Y. Dai, and Y. Xia, “Electrospinning and Electrospun Nanofibers: Methods, Materials, and Applications,” *Chem. Rev.*, vol. 119, 2019, doi: 10.1021/acs.chemrev.8b00593.

[40] B. Araldi da Silva, R. de Sousa Cunha, A. Valério, A. De Noni Junior, D. Hotza, and S. Y. Gómez González, “Electrospinning of cellulose using ionic liquids: An overview on processing and applications,” *Eur. Polym. J.*, vol. 147, p. 110283, 2021, doi: <https://doi.org/10.1016/j.eurpolymj.2021.110283>.

[41] O. Prakash, R. Kumar, A. Mishra, and R. Gupta, “Artocarpus heterophyllus (Jackfruit): An overview,” *Pharmacogn. Rev.*, vol. 3, pp. 353–358, 2009.

[42] T. Chandrasekaran and K. Uppuluri, “Isolation and characterization of cellulose nanocrystals from jackfruit peel,” *Sci. Rep.*, vol. 9, p. 16709, 2019, doi: 10.1038/s41598-019-53412-x.

[43] A. A. S. Raj and T. V. Ranganathan, “Characterization of cellulose from jackfruit (Artocarpus integer) peel,” *J. Pharm. Res.*, vol. 12, no. 3, pp. 311–315, 2018.

- [44] P. K. Sarangi, R. K. Srivastava, A. K. Singh, U. K. Sahoo, P. Prus, and P. Dziekański, “The Utilization of Jackfruit (*Artocarpus heterophyllus* L.) Waste towards Sustainable Energy and Biochemicals: The Attainment of Zero-Waste Technologies,” 2023. doi: 10.3390/su151612520.
- [45] L. Fan, M. M. Gharpuray, and Y.-H. Lee, “Acid Hydrolysis of Cellulose BT - Cellulose Hydrolysis,” L. Fan, M. M. Gharpuray, and Y.-H. Lee, Eds., Berlin, Heidelberg: Springer Berlin Heidelberg, 1987, pp. 121–148. doi: 10.1007/978-3-642-72575-3\_4.
- [46] H. V Lee, S. B. A. Hamid, and S. K. Zain, “Conversion of Lignocellulosic Biomass to Nanocellulose: Structure and Chemical Process,” *Sci. World J.*, vol. 2014, no. 1, p. 631013, 2014, doi: <https://doi.org/10.1155/2014/631013>.
- [47] B. Yang, Z. Dai, S.-Y. Ding, and C. E. Wyman, “Enzymatic hydrolysis of cellulosic biomass,” *Biofuels*, vol. 2, no. 4, pp. 421–449, 2011, doi: 10.4155/bfs.11.116.
- [48] P. Dey, P. Pal, K. Dilip, and D. Das, “Lignocellulosic bioethanol production: Prospects of emerging membrane technologies to improve the process - A critical review,” *Rev. Chem. Eng.*, vol. 36, 2018, doi: 10.1515/revce-2018-0014.
- [49] C. L. Pirich *et al.*, “Influence of mechanical pretreatment to isolate cellulose nanocrystals by sulfuric acid hydrolysis,” *Int. J. Biol. Macromol.*, vol. 130, pp. 622–626, 2019, doi: <https://doi.org/10.1016/j.ijbiomac.2019.02.166>.
- [50] H. Li *et al.*, “Methods to increase the reactivity of dissolving pulp in the viscose rayon production process: a review,” *Cellulose*, vol. 25, 2018, doi: 10.1007/s10570-018-1840-1.

- [51] A. Poulose *et al.*, “Nanocellulose: A fundamental material for science and technology applications,” *Molecules*, vol. 27, no. 22, p. 8032, 2022.
- [52] P. Muley and D. Boldor, *Advances in Biomass Pretreatment and Cellulosic Bioethanol Production Using Microwave Heating*. 2017. doi: 10.18690/978-961-286-048-6.18.
- [53] K. J. Nagarajan *et al.*, “A comprehensive review on cellulose nanocrystals and cellulose nanofibers: Pretreatment, preparation, and characterization,” *Polym. Compos.*, vol. 42, no. 4, pp. 1588–1630, Apr. 2021, doi: <https://doi.org/10.1002/pc.25929>.
- [54] S. Mueller, C. Weder, and E. J. Foster, “Isolation of cellulose nanocrystals from pseudostems of banana plants,” *RSC Adv.*, vol. 4, no. 2, pp. 907–915, 2014, doi: 10.1039/C3RA46390G.
- [55] J. I. Morán, V. A. Alvarez, V. P. Cyras, and A. Vázquez, “Extraction of cellulose and preparation of nanocellulose from sisal fibers,” *Cellulose*, vol. 15, no. 1, pp. 149–159, 2008, doi: 10.1007/s10570-007-9145-9.
- [56] S. Camarero Espinosa, T. Kuhnt, E. J. Foster, and C. Weder, “Isolation of Thermally Stable Cellulose Nanocrystals by Phosphoric Acid Hydrolysis,” *Biomacromolecules*, vol. 14, no. 4, pp. 1223–1230, 2013, doi: 10.1021/bm400219u.
- [57] Y. Sun *et al.*, “Hydrolysis of Cotton Fiber Cellulose in Formic Acid,” *Energy & Fuels*, vol. 21, no. 4, pp. 2386–2389, 2007, doi: 10.1021/ef070134z.
- [58] N. S. Mosier, A. Sarikaya, C. M. Ladisch, and M. R. Ladisch, “Characterization of Dicarboxylic Acids for Cellulose Hydrolysis,” *Biotechnol. Prog.*, vol. 17, no. 3, pp. 474–480, 2001, doi: <https://doi.org/10.1021/bp010028u>.

- [59] A. Samrot *et al.*, “Waste-Derived Cellulosic Fibers and Their Applications,” *Adv. Mater. Sci. Eng.*, vol. 2022, pp. 1–13, 2022, doi: 10.1155/2022/7314694.
- [60] S. Xie, X. Zhang, M. P. Walcott, and H. Lin, “Applications of Cellulose Nanocrystals: A Review ,” 2018. doi: 10.30919/es.1803302.
- [61] Y. Zhang, T. P. Shareena Dasari, H. Deng, and H. Yu, “Antimicrobial Activity of Gold Nanoparticles and Ionic Gold,” *J. Environ. Sci. Heal. Part C*, vol. 33, no. 3, pp. 286–327, 2015, doi: 10.1080/10590501.2015.1055161.
- [62] V. K. Sharma, R. A. Yngard, and Y. Lin, “Silver nanoparticles: Green synthesis and their antimicrobial activities,” *Adv. Colloid Interface Sci.*, vol. 145, no. 1, pp. 83–96, 2009, doi: <https://doi.org/10.1016/j.cis.2008.09.002>.
- [63] K. N Madlum, E. Jasim Khamees, S. Abdulridha Ahmed, and R. Akram Naji, “Antimicrobial and cytotoxic activity of platinum nanoparticles synthesized by laser ablation technique,” *J. Nanostructures*, vol. 11, no. 1, pp. 13–19, 2021.
- [64] C. P. Adams, K. A. Walker, S. O. Obare, and K. M. Docherty, “Size-dependent antimicrobial effects of novel palladium nanoparticles,” *PLoS One*, vol. 9, no. 1, p. e85981, 2014.
- [65] J. Yang, C. Han, F. Xu, and R. Sun, “Simple approach to reinforce hydrogels with cellulose nanocrystals,” *Nanoscale*, vol. 6, no. 11, pp. 5934–5943, 2014.
- [66] H. Golmohammadi, E. Morales-Narváez, T. Naghdi, and A. Merkoçi, “Nanocellulose in sensing and biosensing,” *Chem. Mater.*, vol. 29, no. 13, pp. 5426–5446, 2017.
- [67] R. A. Ilyas, S. M. Sapuan, M. L. Sanyang, M. R. Ishak, and E. S.

Zainudin, “Nanocrystalline cellulose as reinforcement for polymeric matrix nanocomposites and its potential applications: a review,” *Curr. Anal. Chem.*, vol. 14, no. 3, pp. 203–225, 2018.

[68] F. V Ferreira, I. F. Pinheiro, R. F. Gouveia, G. P. Thim, and L. M. F. Lona, “Functionalized cellulose nanocrystals as reinforcement in biodegradable polymer nanocomposites,” *Polym. Compos.*, vol. 39, pp. E9–E29, 2018.

[69] Y. Tang, Z. He, J. A. Mosseler, and Y. Ni, “Production of highly electro-conductive cellulosic paper via surface coating of carbon nanotube/graphene oxide nanocomposites using nanocrystalline cellulose as a binder,” *Cellulose*, vol. 21, no. 6, pp. 4569–4581, 2014, doi: 10.1007/s10570-014-0418-9.

[70] S. Seyednejhad, M. A. Khalilzadeh, D. Zareyee, H. Sadeghifar, and R. Venditti, “Cellulose nanocrystal supported palladium as a novel recyclable catalyst for Ullmann coupling reactions,” *Cellulose*, vol. 26, no. 8, pp. 5015–5031, 2019, doi: 10.1007/s10570-019-02436-7.

[71] P. Dhar, A. Kumar, and V. Katiyar, “Fabrication of cellulose nanocrystal supported stable Fe(0) nanoparticles: a sustainable catalyst for dye reduction, organic conversion and chemo-magnetic propulsion,” *Cellulose*, vol. 22, no. 6, pp. 3755–3771, 2015, doi: 10.1007/s10570-015-0759-z.

[72] A. Percot, C. Viton, and A. Domard, “Optimization of Chitin Extraction from Shrimp Shells,” *Biomacromolecules*, vol. 4, no. 1, pp. 12–18, 2003, doi: 10.1021/bm025602k.

[73] M. Pakizeh, A. Moradi, and T. Ghassemi, “Chemical extraction and modification of chitin and chitosan from shrimp shells,” *Eur. Polym. J.*, vol. 159, p. 110709, 2021, doi: <https://doi.org/10.1016/j.eurpolymj.2021.110709>.

- [74] P. Innocenzi and L. Stagi, “Carbon dots as oxidant-antioxidant nanomaterials, understanding the structure-properties relationship. A critical review,” *Nano Today*, vol. 50, p. 101837, 2023.
- [75] Y. Liu, J. Wei, X. Yan, M. Zhao, C. Guo, and Q. Xu, “Barium charge transferred doped carbon dots with ultra-high quantum yield photoluminescence of 99.6% and applications,” *Chinese Chem. Lett.*, vol. 32, no. 2, pp. 861–865, 2021.
- [76] R. Atchudan, T. N. J. I. Edison, K. R. Aseer, S. Perumal, N. Karthik, and Y. R. Lee, “Highly fluorescent nitrogen-doped carbon dots derived from *Phyllanthus acidus* utilized as a fluorescent probe for label-free selective detection of Fe<sup>3+</sup> ions, live cell imaging and fluorescent ink,” *Biosens. Bioelectron.*, vol. 99, pp. 303–311, 2018.
- [77] L. Zhou, F. Wu, J. Yu, Q. Deng, F. Zhang, and G. Wang, “Titanium carbide (Ti<sub>3</sub>C<sub>2</sub>Tx) MXene: a novel precursor to amphiphilic carbide-derived graphene quantum dots for fluorescent ink, light-emitting composite and bioimaging,” *Carbon N. Y.*, vol. 118, pp. 50–57, 2017.
- [78] H. Ma *et al.*, “Facile synthesis of fluorescent carbon dots from *Prunus cerasifera* fruits for fluorescent ink, Fe<sup>3+</sup> ion detection and cell imaging,” *Spectrochim. Acta Part A Mol. Biomol. Spectrosc.*, vol. 213, pp. 281–287, 2019.
- [79] D. Li *et al.*, “Fluorescent carbon dots derived from Maillard reaction products: their properties, biodistribution, cytotoxicity, and antioxidant activity,” *J. Agric. Food Chem.*, vol. 66, no. 6, pp. 1569–1575, 2018.
- [80] S. Baliyan *et al.*, “Determination of antioxidants by DPPH radical scavenging activity and quantitative phytochemical analysis of *Ficus religiosa*,” *Molecules*, vol. 27, no. 4, p. 1326, 2022.

[81] Y. Hu, L. Tang, Q. Lu, S. Wang, X. Chen, and B. Huang, “Preparation of cellulose nanocrystals and carboxylated cellulose nanocrystals from borer powder of bamboo,” *Cellulose*, vol. 21, no. 3, pp. 1611–1618, 2014, doi: 10.1007/s10570-014-0236-0.

[82] X. F. Sun, F. Xu, R. C. Sun, P. Fowler, and M. S. Baird, “Characteristics of degraded cellulose obtained from steam-exploded wheat straw,” *Carbohydr. Res.*, vol. 340, no. 1, pp. 97–106, 2005, doi: <https://doi.org/10.1016/j.carres.2004.10.022>.

[83] F. T. Seta *et al.*, “Preparation and characterization of high yield cellulose nanocrystals (CNC) derived from ball mill pretreatment and maleic acid hydrolysis,” *Carbohydr. Polym.*, vol. 234, p. 115942, 2020, doi: <https://doi.org/10.1016/j.carbpol.2020.115942>.

[84] F. Yeganeh, R. Behrooz, and M. Rahimi, “The effect of Sulfuric acid and Maleic acid on characteristics of nano-cellulose produced from waste office paper,” *Int. J. Nano Dimens.*, vol. 8, no. 3, pp. 206–215, 2017.

[85] S. Rashid and H. Dutta, “Characterization of nanocellulose extracted from short, medium and long grain rice husks,” *Ind. Crops Prod.*, vol. 154, p. 112627, 2020, doi: <https://doi.org/10.1016/j.indcrop.2020.112627>.

[86] Y. W. Chen, H. V. Lee, and S. B. Abd Hamid, “Facile production of nanostructured cellulose from *Elaeis guineensis* empty fruit bunch via one pot oxidative-hydrolysis isolation approach,” *Carbohydr. Polym.*, vol. 157, pp. 1511–1524, 2017, doi: <https://doi.org/10.1016/j.carbpol.2016.11.030>.

[87] R. Rampazzo, D. Alkan, S. Gazzotti, M. A. Ortenzi, G. Piva, and L.

Piergiovanni, “Cellulose Nanocrystals from Lignocellulosic Raw Materials, for Oxygen Barrier Coatings on Food Packaging Films,” *Packag. Technol. Sci.*, vol. 30, no. 10, pp. 645–661, 2017, doi: <https://doi.org/10.1002/pts.2308>.

[88] F. Li, P. Biagioni, M. Finazzi, S. Tavazzi, and L. Piergiovanni, “Tunable green oxygen barrier through layer-by-layer self-assembly of chitosan and cellulose nanocrystals,” *Carbohydr. Polym.*, vol. 92, no. 2, pp. 2128–2134, 2013, doi: <https://doi.org/10.1016/j.carbpol.2012.11.091>.

[89] S. Azizi, M. Bin Ahmad, N. A. Ibrahim, M. Z. Hussein, and F. Namvar, “Preparation and properties of poly(vinyl alcohol)/chitosan blend bio-nanocomposites reinforced by cellulose nanocrystals,” *Chinese J. Polym. Sci.*, vol. 32, no. 12, pp. 1620–1627, 2014, doi: 10.1007/s10118-014-1548-0.

[90] A. B. Perumal, P. S. Sellamuthu, R. B. Nambiar, and E. R. Sadiku, “Development of polyvinyl alcohol/chitosan bio-nanocomposite films reinforced with cellulose nanocrystals isolated from rice straw,” *Appl. Surf. Sci.*, vol. 449, pp. 591–602, 2018.

[91] A. Thirumalai, A. Girigowami, and K. Girigowami, “Bacterial nanocellulose-Robust preparation and application—A literature review,” *Appl. Chem. Eng.*, vol. 6, 2023, doi: 10.24294/ace.v6i3.2170.

[92] F. Han Lyn and Z. A. Nur Hanani, “Effect of lemongrass (*Cymbopogon citratus*) essential oil on the properties of chitosan films for active packaging,” *J. Packag. Technol. Res.*, vol. 4, pp. 33–44, 2020.

[93] K. V Neenu *et al.*, “Bioactive Cellulose Nanopapers Impregnated With Cinnamon Essential Oil For Sustainable Antibacterial Packaging And Extended Shelf Life Of Coriander Leaves,” 2023.

[94] S. Jancy, R. Shruthy, and R. Preetha, “Fabrication of packaging film reinforced with cellulose nanoparticles synthesised from jack fruit non-edible part using response surface methodology,” *Int. J. Biol. Macromol.*, vol. 142, pp. 63–72, 2020, doi: <https://doi.org/10.1016/j.ijbiomac.2019.09.066>.

[95] L. Fang and J. Zheng, “Carbon quantum dots: Synthesis and correlation of luminescence behavior with microstructure,” *New Carbon Mater.*, vol. 36, no. 3, pp. 625–631, 2021, doi: [https://doi.org/10.1016/S1872-5805\(21\)60031-8](https://doi.org/10.1016/S1872-5805(21)60031-8).

[96] S. R. Joseph, S. Danti, L. Sebastian, and N. VS, “Sustainable innovations: chitosan-cellulose nanocrystal composites for enhanced mechanical, antibacterial, and photocatalytic applications,” *Biomass Convers. Biorefinery*, pp. 1–17, 2024.

[97] R. Ramdani *et al.*, “Curcumin-Laden Crosslinked Chitosan–PVA Films: The Synergistic Impact of Genipin and Curcumin on Accelerating Wound Closure,” *JOM*, vol. 75, no. 12, pp. 5581–5590, 2023.

[97] Z. Li, X. Yang, W. Li, and H. Liu, “Stimuli-responsive cellulose paper materials,” *Carbohydr. Polym.*, vol. 210, pp. 350–363, 2019, doi: <https://doi.org/10.1016/j.carbpol.2019.01.082>.

[98] A. A. Bunaciu, E. gabriela Udriștioiu, and H. Y. Aboul-Enein, “X-Ray Diffraction: Instrumentation and Applications,” *Crit. Rev. Anal. Chem.*, vol. 45, no. 4, pp. 289–299, 2015, doi:

10.1080/10408347.2014.949616.

[99] A. Ganesan, Alaguthirumurugan, T. Sathishkumar, K. Kuppamuthu, and R. Jaiganesh, “Strategy Towards Active Food Packaging Material From Cellulose Nanoparticles and its Characterization,” *Lett. Appl. NanoBioScience*, 2021, doi: 10.33263/LIANBS114.42554262.

[100] C. D. Midhun Dominic *et al.*, “Colocasia esculenta stems for the isolation of cellulose nanofibers: a chlorine-free method for the biomass conversion,” *Biomass Convers. Biorefinery*, vol. 14, no. 9, pp. 10305–10318, 2024, doi: 10.1007/s13399-022-03171-z.

[101] A. Dutta, “Chapter 4 - Fourier Transform Infrared Spectroscopy,” in *Micro and Nano Technologies*, S. Thomas, R. Thomas, A. K. Zachariah, and R. K. B. T.-S. M. for N. C. Mishra, Eds., Elsevier, 2017, pp. 73–93. doi: <https://doi.org/10.1016/B978-0-323-46140-5.00004-2>.

[102] A. Mohammed and A. Abdullah, “Scanning electron microscopy (SEM): A review,” in *Proceedings of the 2018 International Conference on Hydraulics and Pneumatics—HERVEX, Băile Govora, Romania*, 2018, pp. 7–9.

[103] C. Y. Tang and Z. Yang, “Chapter 8 - Transmission Electron Microscopy (TEM),” N. Hilal, A. F. Ismail, T. Matsuura, and D. B. T.-M. C. Oatley-Radcliffe, Eds., Elsevier, 2017, pp. 145–159. doi: <https://doi.org/10.1016/B978-0-444-63776-5.00008-5>.

[104] C. De Blasio, “Thermogravimetric Analysis (TGA) BT - Fundamentals of Biofuels Engineering and Technology,” C. De Blasio, Ed., Cham: Springer International Publishing, 2019, pp. 91–

102. doi: 10.1007/978-3-030-11599-9\_7.

[105] K. V Neenu *et al.*, “Effect of oxalic acid and sulphuric acid hydrolysis on the preparation and properties of pineapple pomace derived cellulose nanofibers and nanopapers,” *Int. J. Biol. Macromol.*, vol. 209, pp. 1745–1759, 2022, doi: <https://doi.org/10.1016/j.ijbiomac.2022.04.138>.

[106] J. Pelleg, *Mechanical properties of materials*, vol. 190. Springer, 2013.

[107] P. Lu and Y.-L. Hsieh, “Preparation and properties of cellulose nanocrystals: rods, spheres, and network,” *Carbohydr. Polym.*, vol. 82, no. 2, pp. 329–336, 2010.

[108] N. El Miri *et al.*, “Bio-nanocomposite films based on cellulose nanocrystals filled polyvinyl alcohol/chitosan polymer blend,” *J. Appl. Polym. Sci.*, vol. 132, no. 22, 2015.

[109] K. Sreekanth, K. P. Sharath, M. D. CD, D. Mathew, and E. K. Radhakrishnan, “Microbial load reduction in stored raw beef meat using chitosan/starch-based active packaging films incorporated with cellulose nanofibers and cinnamon essential oil,” *Meat Sci.*, vol. 216, p. 109552, 2024.

[110] J. Xu, R. Xia, L. Zheng, T. Yuan, and R. Sun, “Plasticized hemicelluloses/chitosan-based edible films reinforced by cellulose nanofiber with enhanced mechanical properties,” *Carbohydr. Polym.*, vol. 224, p. 115164, 2019, doi: <https://doi.org/10.1016/j.carbpol.2019.115164>.

*References*

---

## *Papers published/Presented*

---

1. Conference proceedings: Teresian Centenary International Multidisciplinary Conclave – 2024 (TCIMC – 2024) – Feba George T. -16<sup>th</sup> December, 2024

Title: “Valorizing Jackfruit Peel Waste into High-Performance Cellulose Nanocrystals for Environmental Remediation and Sustainable Packaging”

2. Poster Presentation: National Seminar on “Ethnic Medicine – A Chemical Perspective” as part of Albertian Knowledge Summit : An International Conference on Multidisciplinary Research at St. Albert’s College (Autonomous), Ernakulam - Feba George T. – 12<sup>th</sup> February, 2025

Title: “Green Composites from Shrimp Shells and Jackfruit Peels for Hydrocarbon Removal in the Cochin Estuary”